Russian Chemical Reviews **72** (2) 123 – 141 (2003) © 2003 Russian Academy of Sciences and Turpion Ltd

DOI 10.1070/RC2003v072n02ABEH000789

Single-layer dispersions of transition metal dichalcogenides in the synthesis of intercalation compounds

A S Golub, Ya V Zubavichus, Yu L Slovokhotov, Yu N Novikov

Contents

I.	Introduction	123
II.	Characteristic features of the layered metal chalcogenide structures	123
III.	Solid-phase intercalation of metal dichalcogenides and the types of their intercalation compounds	125
IV.	Single-layer dispersions of metal dichalcogenides	128
V.	Layered compounds obtained from single-layer dispersions	129
VI.	Structural transformations of the chalcogenide matrices in the formation of single-layer dispersions	135
VII.	Possible applications of the materials obtained with the use of single-layer dispersions	138
VIII.	Conclusion	138

Abstract. Chemical methods for the exfoliation of transition metal dichalcogenides in a liquid medium to give single-layer dispersions containing quasi-two-dimensional layers of these compounds are surveyed. Data on the structure of dispersions and their use in the synthesis of various types of heterolayered intercalation compounds are discussed and described systematically. Structural features, the electronic structure and the physicochemical properties of the resulting intercalation compounds are considered. The potential of this method of synthesis is compared with that of traditional solid-state methods for the intercalation of layered crystals. The bibliography includes 192 references.

I. Introduction

A crystal structure of layered transition metal dichalcogenides TX_2 consists of the alternating infinite triatomic layers X – T – X (where T is a transition metal atom, X is a chalcogen atom — S, Se or Te).[1] The neighbouring metal and chalcogen atoms are strongly bound by covalent bonds within the layers, while the layers are weakly bonded to each other due to van der Waals interactions. These compounds have found practical applications as materials used in electronics (*e.g.*, in power sources), in different fields of technology (*e.g.*, as lubricants) and in petrochemistry (as catalysts). They also attract attention in the fundamental research of physical and chemical properties of the low-dimensional compounds.

Approaches common to dichalcogenides of different metals can be used in studies (and for the modification) of their properties, because of their structural similarity. One of the approaches makes use of the ability of these substances to form intercalation compounds due to the existence of the interlayer space between the adjacent TX_2 layers. This allows one to obtain systems with alternating TX_2 monolayers and layers of different (inorganic or organic) nature. In such heterolayered structures both the electronic structures and the properties of the TX_2 layers can be modified due to charge transfer between the components and changes in the nature and concentrations of intercalated substances (which consequently changes interlayer distances).

An unusual chemical property of transition metal dichalcogenides discovered recently is their ability to form rather stable systems containing quasi-two-dimensional monomolecular layers separated by the solvent molecules (single-layer dispersions). To some extent, this property is analogous to the ability of layered aluminosilicates and zirconium hydrogen phosphates[2] to exfoliate in aqueous media. A general character of this phenomenon for the layered systems can be supposed, and based on this a versatile method can be developed for the preparation of intercalation compounds and nanocomposite materials including films.

This method is of particular importance for the synthesis of heterolayered systems that cannot be obtained by traditional procedures of solid-state chemistry. In this respect, formulation of the basic principles of the synthesis of intercalation compounds with the use of TX_2 single-layer dispersions is the subject of current interest, and the present review is expected to provide additional insights into the problem.

In this review, the data on the nature of TX_2 single-layer dispersions and their use in the synthesis of new heterolayered materials as well as the data on the types, properties and structural features of these materials published in the few last years are considered. To reveal the reactivity of the single-layer dispersions, it was appropriate to compare it with that of the solid-state intercalation reactions of crystalline layered metal dichalcogenides. It should be mentioned that different aspects of solid-phase intercalation were discussed in several reviews published in the 1980 – 1990's (see, *e.g.*, Refs 3 – 9), while the studies of single-layer dispersions have up to now been surveyed in only one review[10] dealing with molybdenum disulfide chemistry.

II. Characteristic features of the layered metal chalcogenide structures

Many transition metals characterised by the oxidation state +4 [Group IVB, VB and VIB metals and some Group VIIB (Tc, Re) and VIIIB (Pt) metals] form dichalcogenides of the layered

A S Golub, Ya V Zubavichus, Yu L Slovokhotov, Yu N Novikov
A N Nesmeyanov Institute of Organoelement Compounds, Russian Academy of Sciences, ul. Vavilova 28, 119991 Moscow, Russian Federation. Fax (7-095) 135 50 85.
Tel. (7-095) 135 93 26. E-mail: golub@ineos.ac.ru (A S Golub).
Tel. (7-095) 135 93 04. E-mail: Yan.Zubavichus@urz.uni-heidelberg.de (Ya V Zubavichus), slov@ineos.ac.ru (Yu L Slovokhotov).
Tel. (7-095) 135 92 13. E-mail: novik@ineos.ac.ru (Yu N Novikov)

Received 25 October 2002
Uspekhi Khimii **72** (2) 138 – 158 (2003); translated by A S Golub

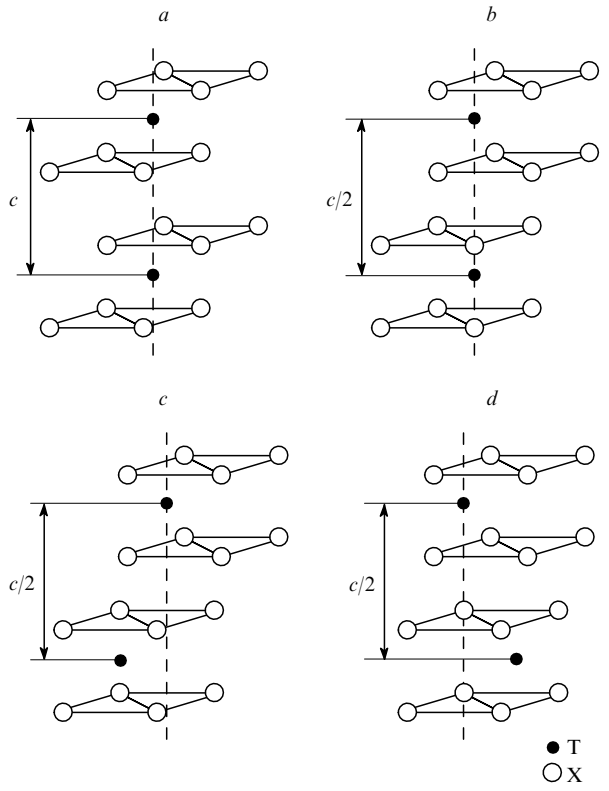


Figure 1. The main types of crystal structures of transition metal dichalcogenides.
Polytypes: (*a*) 1T, (*b*) $2H_a$, (*c*) $2H_b$, (*d*) $2H_c$.

structure.[1] Their crystal structure can be described as stacking of closely packed hexagonal sheets of chalcogenide anions with each second interlayer space occupied by metal atoms (Fig. 1). With the close packing, the stacking of the anions accords with the principle 'an atom is placed over the centre of the triangle formed by the atoms of the adjacent layer', and this principle is held in all cases where the adjacent chalcogen sheets with no metal atoms in between are stacked and bound to each other only by the van der Waals forces (to form a van der Waals gap). This arrangement causes the existence of octahedral and tetrahedral vacant sites in the ratio of 1 : 2 in the interlayer space between the neighbouring triatomic X−T−X···X−T−X layers. The electron configuration of the metal atom T determines the intralayer mutual arrangement of the chalcogen sheets and specifies its octahedral (which corresponds to the close packing of the anions) or trigonal prismatic (where the packing of the anions is not close) nearest-neighbour surrounding the chalcogen atoms. According to quantum-chemical calculations,[11–13] a trigonal prismatic coordination is favoured by a d^2 metal atom electron configuration (the Group VIB metals, Mo and W) while the octahedral coordination is characteristic of a d^0 metal atom configuration (Group IVB metals, Ti and Zr). For the Group VB metals (Nb and Ta) with d^1 electron configuration, both coordination surroundings are energetically close to each other. For this reason, both trigonal prismatic and octahedral coordinations are usually present in real structures.

In addition to the type of coordination polyhedron (octahedron or trigonal prism), the motives of the X−T−X layer packing can vary as well as the relative positions of the metal cations in the adjacent layers with respect to each other in the structures of metal dichalcogenides.[14] These three factors taken together determine the syngony [hexagonal (H), trigonal (T) or rhombohedral (R)] and the space group of the crystalline compound. Thus in the case of an octahedrally surrounded metal atom, the sole one-layered packing, which corresponds to the trigonal space group $P3m$ (1T polymorph), is realised. In the case of trigonal prismatic coordination, much more variation in the packing exist. For two-layered packing, three structural types differing in the relative positions of the metal cations in the adjacent filled layers are possible (2H polymorph, $2H_a$, $2H_b$ and $2H_c$ polytypes).[3] Three-, four- and six-layered sequences in packing as well as more exotic long-period structures are also known. Some compounds exhibit structures with a mixed coordination environment. They contain alternating layers with octahedral and trigonal prismatic nearest-neighbour surrounding of a metal atom.[1,3] The main polymorph modifications and polytypes of layered dichalcogenides are listed in Table 1 and schematically depicted in Fig. 1.

Table 1. Structural types of transition metal dichalcogenides.[3]

Polymorph	Polytype	Coordination type	Layer stacking motif[a]	Space group	Examples
1T	1T	O	AbC	$P\bar{3}m$	TiS_2, VS_2, TaS_2
2H	$2H_a$	TP	AbACbC	$P6_3/mmc$	NbS_2, TaS_2
	$2H_b$	TP	AbABcB	$P6m2$	$NbSe_2$, $TaSe_2$
	$2H_c$	TP	AbABaB	$P6_3/mmc$	MoS_2, WS_2
3R	3R	TP	AbACaCBcB	$R3m$	MoS_2, WS_2
4H	$4H_a$	TP	BcBAcABcBCaC	$P\bar{6}m2$	$NbSe_2$, $TaSe_2$
	$4H_b$	O + TP	BcBCaBCaCBaC	$P6_3/mmc$	TaS_2, $TaSe_2$
	$4H_c$	TP	BcBAcABaBCaC	$P6_3mc$	$TaSe_2$
6R	6R	O + TP	BcBCaBCaCAbCAbABcA	$R3m$	TaS_2, $TaSe_2$

Note. The following notations are used: O, octahedral coordination; TP, trigonal prismatic coordination; O + TP, mixed coordination.
[a] Upper- and lower-case letters designate the location of the chalcogen and metal atoms, respectively. Coincidence of the letters corresponds to the situation where the atoms in the adjacent layers are disposed exactly one below the other.

The electronic structures of layered dichalcogenides TX_2 are also determined by the nature of the metal T. The TX_2 valence band structure was found to consist of two sub-bands, where the lower sub-band is composed mainly by *n*s- and the upper sub-band by *n*p-states of the chalcogen atom ($n = 3$ for X = S and $n = 4$ for X = Se) (Fig. 2). The lower free states of the vacant band (conduction band) consist mainly of d-orbitals of the transition metal. Due to the splitting of d-orbitals of the metal T by a crystal field of the chalcogen, the d_{z^2}-orbital becomes the lowest in energy and forms a separate sub-band. In the case of Group IVB metal chalcogenides (d^0 configuration), this orbital is situated entirely in the vacant band, whereas for Group VB metal chalcogenides (d^1 configuration) this orbital is half-filled, and for Group VIB metal dichalcogenides (d^2 configuration), the d_{z^2}-orbital is completely occupied and lies in the valence band.[11,15–17] Thus, according to the calculations and experimental data [measurements of conductivity, magnetic properties,[18,19] photoelectonic spectra,[17,20] X-ray absorption near-edge structure (XANES),[21] and optical reflection spectra [22]], the occupied and vacant levels are separated by a very narrow energy gap (0.1–0.2 eV) in 1T-TiS_2, while they overlap in 2H-TaS_2. In 2H-MoS_2 and 2H-WS_2, the energy gap reaches $\sim$ 1.5 eV.

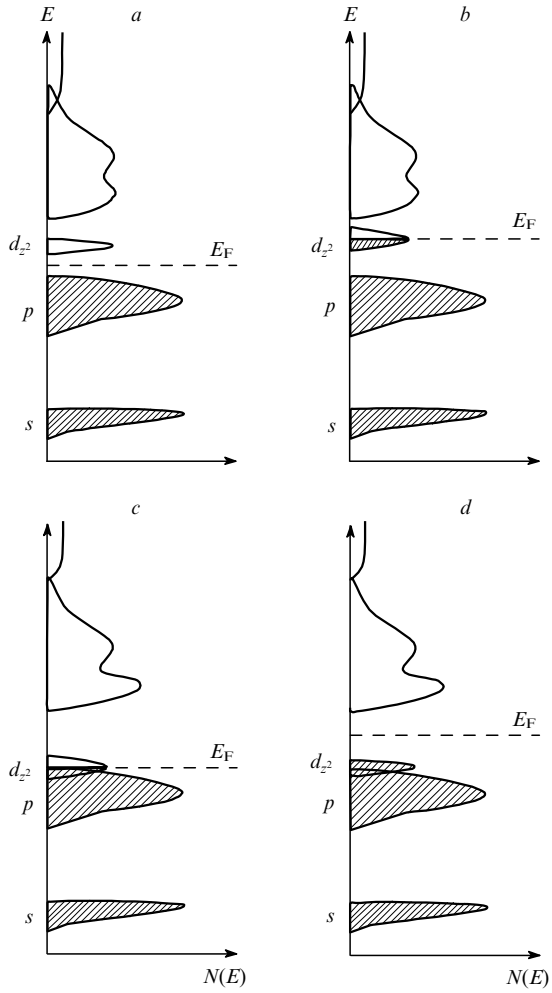


Figure 2. Band structures for dichalcogenides of Group IVB (*a*), VB (*b*, *c*) and VIB (*d*) transition metals with octahedral (*a*, *b*) and trigonal prismatic (*c*, *d*) coordination of the central atom.[11]

Let us consider the structure of MoS_2 in more detail, because this compound is inert in solid-state intercalation reactions, and it is the most common subject of studies on single-layer dispersion phenomenon. Molybdenum disulfide is a unique naturally occurring layered metal dichalcogenide. The mineral molybdenite contains its most stable 2H-modification ($2H_c$ polytype, see Table 1), which has two-layered packing AbABaB with a trigonal prismatic coordination of molybdenum atoms [the space group $P6_3/mmc$, $a = 3.16$ Å, $c = 12.30$ Å, $Z = 2$ (see Ref. 23)]. Another thermodynamically stable modification of MoS_2 is 3R, which is characterised by three-layered packing and also has a trigonal prismatic coordination of molybdenum atoms [space group $R3m$, $a = 3.16$ Å, $c = 18.37$ Å, $Z = 3$ (see Ref. 24)]. Virtually amorphous molybdenum disulfide consisting of strongly disordered fragments of the 2H structure can be obtained by ion-exchange reactions of molybdenum chloride with alkali metal sulfides in non-aqueous solvents.[25] Recently, the preparation of molybdenum disulfide in the form of multi-layered polyhedral structures, resembling carbon 'onions' and nanotubes, by sulfidation of ultradispersed molybdenum oxide[26,27] or by reduction of MoS_3 with hydrogen has been reported.[28] Though today the atomic structures of these systems are not known in detail, they are presumably close to the 2H-modification and have a certain number of defects needed for deformation of the flat S–Mo–S layer to the given curvature. The minimum diameter of such MoS_2 particles (containing 2–3 layers) is approximately 30–50 Å.[29] Flat one-layered nanosized MoS_2 clusters of approximately the same diameter have been obtained by the reaction of $MoCl_4$ with H_2S in a micellar solution.[30]

Synthesis of a metastable molybdenum disulfide modification, in which the octahedral coordination of molybdenum atoms and one-layered packing are assumed, has been reported.[31] This modification can be assigned to the 1T polymorph (see Table 1). For the synthesis of this compound, the intercalation compound $K_{0.7}MoS_2$ was subjected to controlled hydrolysis up to the composition of $K_{0.33}(H_2O)_{0.6}MoS_2$ followed by its electrochemical or chemical oxidation (using potassium dichromate in dilute sulfuric acid or iodine in acetonitrile). According to the powder X-ray diffraction analysis, the structure of the obtained compound belongs to a hexagonal syngony and has the unit cell dimensions $a = 5.597$ Å, $c = 5.994$ Å.[31] The structure is characterised by a shorter interlayer distance (by ~ 0.16 Å) than 2H-MoS_2, and by the existence of a superstructure $\sqrt{3}a \times \sqrt{3}a$ in the *ab* plane of the layer. This compound possesses a negative temperature coefficient of electronic conductivity and exhibits the Pauli paramagnetism, *i.e.*, displays metallic properties. Thermal analysis showed that decomposition of the compound proceeds at ~ 100 °C with a small exothermic effect resulting in the formation of strongly disordered 2H-MoS_2. The structural study of 1T-MoS_2 by electronography[32] confirmed the retention of a hexagonal symmetry of the MoS_2 layer and the formation of the superstructure $\sqrt{3}a \times \sqrt{3}a$ due to the displacement of the molybdenum atoms from their ideal positions in the layer. This structural model is consistent with the data from scanning tunneling microscopy[33] and with the results of quantum-chemical calculations.[34] Nevertheless, since the atomic structure of the MoS_2 modification under consideration has not been determined up to now, the notation '1T-modification' has to be used with care. In particular, '1T-MoS_2' was suggested[35] to be a product of proton insertion into molybdenum disulfide — $H_x^+(MoS_2)^{x-}$. (Similar intercalation compounds with hydrogen are known for some chalcogenides of the Group VB metals.[36,37])

III. Solid-phase intercalation of metal dichalcogenides and the types of their intercalation compounds

In the literature, TX_2 intercalation compounds with various electron donors such as alkali metals and their complexes with solvating molecules, transition and post-transition metals, organic molecules (Lewis bases) and metal complexes of low ionisation potentials are described. The main traditional methods applied for the intercalation of powdered crystalline dichalcogenides, TX_2, are as follows: thermally activated insertion of the guest (metal atoms, molecules of electron-donating substances) into the TX_2 interlayer space, intercalation under electrolysis conditions where TX_2 is used as a cathode, and, in the case of alkali metals, the action of reducing agents (for instance, n-butyllithium or $NaBH_4$) on TX_2. The early publications concerning the methods of synthesis and the structures of certain classes of intercalation compounds are summarised in several reviews (see, for example, Ref. 3–6, 38).

It has been repeatedly noticed that the crystals of Group IVB and VB metal dichalcogenides can be intercalated by each of the above-mentioned types of the compounds using classical methods of solid-state chemistry, while molybdenum and tungsten dichalcogenides can only be intercalated with alkali metals under the same conditions. The different reactivities of the matrices can be explained by the distinctions in their electronic structures. Actually, taking into account the TX_2 valence band model considered above and in the framework of the rigid band model (RBM) (which is obeyed fairly well for the majority of dichalcogenides), the filling of the vacant matrix levels by the electrons of the guest is expected to proceed most easily in the cases of matrices based on the Group IVB and VB metals and should be most hindered in the case of Group VIB metal dichalcogenides where

d_{z^2}-orbitals are occupied and the electrons have to fill higher non-bonding levels.

According to this model, a new molybdenum disulfide 1T-modification, which exhibits a metal-type conductivity, should be more reactive in the intercalation than 2H-MoS_2. This is consistent with the fact that 1T-MoS_2 udergoes intercalation with metallic mercury [39] as well as with Ag^+ and Cu^+ cations (see Ref. 40).

However, even with TX_2 the electronic structures of which favour the acceptance of electrons, the key step of intercalation that limits the rate of the process, is apparently a transfer of the electrons to the matrix layers. The data on the kinetics of the gas-phase intercalation of hydrazine into $NbSe_2$ [41] as well as of the solution intercalation of cobaltocene into $TaSe_2$ [42] shows that the filling of the interlayer space is preceded by an induction period, which is needed for the 'activation' of the matrix due to its interaction with the absorbed molecules. The limiting influence of this step also follows from the effect of the acceleration of TiS_2 intercalation with various amines upon introduction, in the reaction system, of lithium amides or buthyllithium, which can easily reduce the matrix layers. Probably, activation occurs due to weakening of the layer attraction because of the transfer of a certain number of electrons into the layers, which results in Coulombic repulsion. This facilitates the entering of the cations into the interlayer space.[43]

It is important for the next steps of the process that cations should easily diffuse into the interlayer space, liberating the edge positions for the entering of new atoms or molecules (Fig. 3). The mobilities of compounds intercalated evidently diminish with the increase in their radii and with the augmentation of covalence of the guest–matrix bonding. This causes rather severe conditions for the insertion of many of the guest compounds into the interlayer space, thus limiting the range of compounds that can be intercalated in the crystalline dichalcogenides TX_2.

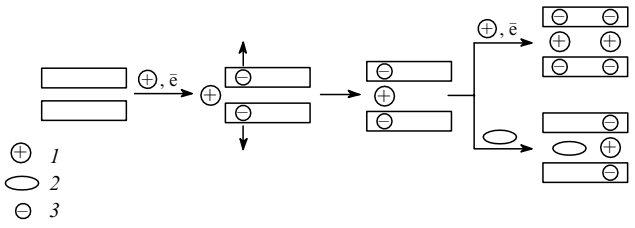


Figure 3. Schematic representation of the activation of a crystalline layered matrix in intercalation reactions;
(*1*) a cation; (*2*) a neutral molecule; (*3*) negative charge on the layer.

1. Compounds with molecular electron donors

In most cases, the intercalation of molecular compounds in the dichalcogenide matrices demands long (often, for many days) heating of a TX_2 powder in contact with a liquid or vaporous intercalant.[3] Steric factors play an important role in this process. For this reason, two-stage synthetic methods are often used. For instance, TaS_2 was intercalated with ammonia, which was then replaced by bulkier molecules of pyridine [44] or n-alkylamines.[45]

Entering of guests in the van der Waals gap leads to a significant increase in the interlayer spacing (Δc), which can vary from 3 Å (in the case of NH_3) to 50 Å (in the case of stearamide),[44] and to the essential lowering of the overall structural ordering of the materials. In the compounds obtained, the interlayer arrangement of the matrix layers is determined by the van der Waals guest–matrix interactions and by the orientation of the guest molecules. Therefore, there are no correlations in the stacking of adjacent matrix layers in these compounds, *i.e.*, the layers are packed turbostratically. In most cases, the guest molecules are almost closely packed in the interlayer space of the matrix, which implies van der Waals guest–guest interaction. As a rule, the periodicity in the guest layer appears quite weakly or not at all in the diffraction pattern.

Intercalation compounds of this type were initially believed to contain only neutral molecules which interact with the matrix due to the overlap of the heteroatom lone pair of the electrons with vacant orbitals of the matrix.[44, 46, 47] Such a viewpoint can sometimes be found in the current literature (see, for instance, Ref. 48) though it contradicts the known data on the substantial electron transfer from an intercalant to the vacant band of the matrix (in particular, up to 0.3 ē per atom of Ta in a compound of TaS_2 with pyridine [49]). Further studies revealed the presence of ions along with neutral particles in the interlayer space. The former are produced in various reactions accompanying the intercalation. For instance, in the case of ammonia intercalation into TaS_2 at 25 °C in the absence of oxygen and water, the formation of molecular nitrogen has been found by mass spectrometry. This suggests the occurence of a redox reaction between the matrix and the intercalant resulting in the formation of ammonium cations, which are intercalated into TaS_2 together with neutral NH_3 molecules (see Ref. 6).

$$TaS_2 \xrightarrow{NH_3} (NH_4^+)_x(NH_3)_y(TaS_2)^{x-} + \frac{x}{6}N_2\,. \qquad (1)$$

The composition of a compound of TiS_2 with ammonia where the cationic species amount to 20% (Ref. 50) can be formulated as $(NH_4^+)_{0.2}(NH_3)_{0.8}(TiS_2)^{0.2-}$. On heating at 147 °C, all the neutral ammonia molecules can be removed and the compound becomes an ammonium analogue of the entirely ionic TX_2 intercalation compounds with alkali metals.

2. Compounds with alkali metals

Alkali metals (A) can be introduced into the interlayer space of crystalline dichalcogenides TX_2 by several methods:

(*1*) from vapour phases of alkali metals;[4]

(*2*) from the alkali metal solutions in liquid ammonia;[38, 51, 52]

(*3*) from the alkali halide melts;[53]

(*4*) by electrochemical intercalation using non-aqueous solutions of alkali metal salts;[38]

(*5*) by the reaction of TX_2 with some alkali metal compounds (Bu^nLi/hexane, ABH_4);[54, 55]

(*6*) by other methods that do not imply direct intercalation.

It should be mentioned that in the cases of heavy alkali metals the vapour-phase synthesis (*1*) is carried out at elevated temperatures, which is accompanied by a side reaction, *viz*., the reduction of TX_2 to a lower chalcogenide with the formation of the corresponding A_2X.[4] In most cases, the method (*2*) allows the preparation of TX_2 intercalation compounds with alkali metals solvated by ammonia.[38] The reduction of alkali metal thiomolybdates, A_2MoS_2, by hydrogen provides example of the synthesis of intercalation compounds according to the method (*6*).[32]

Intercalation compounds A_xTX_2 obtained in these reactions undergo spontaneous hydration in the presence of traces of moisture and self-ignite upon exposure to air. This makes the investigation of their structure and properties very difficult. The available structural data were obtained with polycrystalline samples. The attempts to synthesise single crystals of A_xTX_2 failed. It was noted [56] that single crystals of titanium disulfide were destroyed during intercalation due to strong local stresses and deformations of its layers.

The content of alkali metals in A_xTX_2 varies from 0.3 to 1 atom per T atom depending on the nature of A and the method of preparation. The maximum content of alkali metal ($x \geqslant 1$) has been achieved for A = Li.[57] For all the A_xTX_2 compounds, interlayer spacing augments as the ionic radius of A^+ increases.

Solid-state NMR studies of Li_xTiS_2 showed that the guest atoms are virtually fully ionised in the compounds with alkali metals.[58, 59] Thus, taking into account the maximum stoichiometry of these compounds, charge transfer to the vacant orbitals of the matrix can reach 1 ē per titanium atom. In spite of the fact

that the sulfur atoms are involved in the acceptance of the electron density (XAFS data [21]), this comes mainly to d-orbitals of titanium since they form a lower-energy vacant band. According to X-ray spectroscopic data, this leads to a formal reduction of titanium. Thus, using X-ray emission Ti $K_{\alpha 1}$ spectra it was established [60] that the charge states of titanium in $LiTiS_2$ and in $TiS_{1.5}$ are identical.

Electrophysical properties of the materials are changed in the expected way due to a charge transfer. In particular, the intercalation of Group IVB metal dichalcogenides results in a change in the conductivity character from semi-conducting to metallic. On the contrary, the properties of dichalcogenide phases containing Group VB metals change from metallic to semi-conducting with an increase in the guest metal concentration.[61] Many compounds of this type were found to be superconductors. To our knowledge, the maximum transition temperature ($\sim$ 6.9 K) was found for MoS_2 compounds with rubidium and caesium.[4]

Intercalation with alkali metals cannot always be reduced to mere filling of the vacant tetrahedral or octahedral sites in the initial TX_2 structure since this often triggers structural transformations. For instance, the shift of the S–Ti–S layers one with respect to another occurs upon intercalation of 1T-TiS_2, so that the environment of the guest atoms becomes trigonal prismatic for certain guest : host ratios. A similar structural transition has been described for Na_xTiS_2 and K_xTiS_2.[51]

Yet another type of transformation changing the geometry of the TX_2 layer itself occurs in the intercalation of lithium into 1T-TaS_2. In this case, the transition octahedron – trigonal prism was found to occur in the local environment of tantalum.[62] It seems likely that the reverse change in the T metal coordination is induced by the intercalation of Group VIB metal dichalcogenides with alkali metals. As was found in the study of electrochemical insertion of lithium into 2H-MoS_2, the structural phase transition appeared as a plateau in the voltammogram for the composition $Li_{0.1}MoS_2$.[57] An X-ray diffraction study of the resulting polycrystalline phase with the composition $LiMoS_2$ showed that intercalation of lithium not only leads to an increase in the lattice parameters (a = 3.36 Å, c = 6.30 Å) with respect to those of 2H-MoS_2 (a = 3.16 Å and $c = 2 \times 6.15$ Å), but also changes the layer stacking from the two-layered sequence to one-layered and, consequently, the coordination surrounding the molybdenum atoms from trigonal prismatic to octahedral. For the intercalates with high lithium content (Li_xMoS_2, $x > 1$), electronography revealed the formation of a $2a \times 2a$ superstructure which disappears irreversibly on heating of the sample.[63] This effect was construed to be a consequence of lithium ion ordering within octahedral vacant sites. However, the reason for the appearance of the superstructure reflections is most likely the ordering not only in the intercalated layer, but also in the matrix layers. This viewpoint is supported by the Mo K-edge EXAFS data,[39, 64] which demonstrated significant redistribution of the Mo–Mo bond lengths in $LiMoS_2$, and by the analysis of atomic pair distribution function (PDF) [65] for this compound as well.

Probably, charge transfer from the other guest alkali metals to the MoS_2 matrix layers results in similar changes in these layers. For instance, electron microdiffraction and X-ray powder diffraction studies of the intercalation compound $K_{0.7}MoS_2$ obtained by reduction of potassium thiomolybdate with hydrogen, revealed the existence of a $2a \times 2a$ superstructure in the MoS_2 layer.[32] Taking into consideration the stacking of neighbouring layers, the crystal structure of $K_{0.7}MoS_2$ [also as in the case of $LiMoS_2$ (Ref. 65)] does not have hexagonal symmetry and was described using a triclinic unit cell with the following parameters: $a = b$ = 6.6 Å, c = 8.0 Å, α = 76.2°, β = 88.3°, γ = 60.3° (the space group $P1$).[32]

3. Layered solvates

Layered solvates of the TX_2 intercalation compounds with alkali metals, $A_x(solv)_yTX_2$, can be obtained in the reaction of solvating reagents (water, liquid ammonia, dimethyl sulfoxide, dimethoxyethane, dimethylformamide) with A_xTX_2 or in the direct intercalation reaction, if it is carried out in the required solvent.[66–70] These compounds are of much interest as the direct precursors of single-layer dispersions.

Normally, the content of alkali metals in solvated phases is lower than in the intercalation compounds with the same non-solvated metals. Typical x values lie in the range 0.1–0.33. For this type of compound, the guest and host charges remain separated, *i.e.* the atoms of the alkali metals remain virtually fully ionised. For these compounds, the expansion of interlayer spacing with respect to the interlayer spacing in the initial TX_2 structure depends weakly on the ionic radius of the alkali metal and is mainly determined by the van der Waals thickness of solvating molecules. For this reason, the distance between the adjacent layers may change in a stepwise manner depending on whether the solvating molecules form a monolayer, bilayer *etc*. In the case of water as a solvent, it was found that Li^+ and Na^+ ions, which have a high energy of hydration (the ions characterised by the ratio $n/r \geqslant 1$, where n is the cation charge, r is the ionic radius /Å), tend to form intercalation compounds containing two water layers, whereas all the other cations stabilise only one-layered packing of water in the interlayer space (Fig. 4).[66, 71]

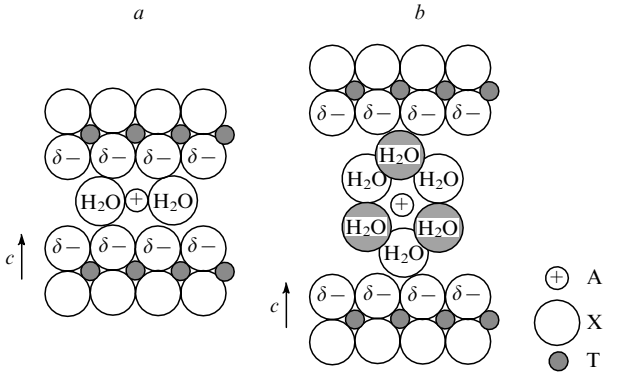


Figure 4. Coordination of the intercalated alkali metal cation with water molecules arranged in one-layer (*a*) or bilayer (*b*) packing in compounds $A_x(H_2O)_yTX_2$.[71]

For the majority of layered solvates, only a periodicity in the direction normal to the layers was determined by structural metods. Structural data are known in greater detail only for the isolated examples. One of them represents the intercalation compound $K_{0.33}(H_2O)_{0.66}MoS_2$, which has a monoclinic unit cell with the parameters a = 5.70 Å, b = 3.24 Å, c = 9.46 Å, β = 100.5° as was found by XRPD and electron microdiffraction methods.[31,32] Thus, the interlayer spacing in this compound is larger than in 2H-MoS_2 by 3.15 Å, which is close to the van der Waals thickness of the monolayer of water molecules.

For the series of intercalation compounds $A_x(H_2O)_yMoS_2$ (A = Li, Na, K, Cs), the ordering and dynamic behaviour of water molecules and alkali metal cations have been investigated by magic-angle-spinning NMR (^{1}H, ^{7}Li, ^{23}Na, ^{133}Cs).[71] It was found that alkali metal cations have a strongly distorted octahedral environment and that water molecules possess high mobility in the intercalated layer where their chaotic motion can be observed even at 20 °C.

In these compounds, the cations of alkali metals can be involved in ion-exchange reactions (for instance, with alkylammonium cations) giving rise to new intercalation compounds.[67]

4. Compounds with transition and post-transition metals

Compounds with the composition M_xTX_2 (M is a 3d-metal, Cu, Ag *etc*.) are usually obtained by thermal synthesis at 600–1100 °C in tubes containing a mixture of TX_2 and M or a mixture of three elements T, M and X in the appropriate stoichiometry. Note that

this reaction, in particular, in the latter combination, can hardly be considered as the intercalation of a layered matrix. However, the compositions of these ternary metal chalcogenides can be considered as intercalation compounds from the structural point of view, because the host matrix and the guest layers can be distinguished in their structure. Due to strong covalence of the M–X bond, the accommodation of M atoms in the interstitial sites of these compounds results in a small increase or, for some 3d-metals (Co, Ni), even in a decrease in the interlayer distance.[72] The crystallinity of M_xTX_2 compounds is usually high. Using gas-transport reactions (for instance, in the presence of iodine or chlorine), single crystals of $Co_{0.25}TiS_2$,[73] $Fe_{0.34}TiSe_2$,[74] $Ag_{0.6}NbS_2$ (Ref. 75) and $In_{0.67}TaS_2$ (Ref. 76) could be grown.

In most M_xTX_2 compounds described, the guest M atoms are localised in the octahedral sites formed by chalcogen atoms of the adjacent layers, though filling of the tetrahedral sites is also known [Cu, Ag (see Ref. 77)]. Ultimate concentration of the guest atoms in M_xTX_2 is limited not only by the number of available sites, but also by the 'capacity' of the d_{z^2}-sub-band part, which is vacant in the non-intercalated matrix. According to RBM, this sub-band can adopt 2 and 1 $\bar{e}$ per T atom in cases of Group IVB and VB metal dichalcogenides, respectively. Actually, the maximum x values found experimentally for M_xTX_2 are close to the expected values. For instance, the x values are equal to 0.75 and 0.5 for TiS_2 and NbS_2, respectively,[78,79] when they are intercalated with 3d-metals (Mn, Fe, Co, Ni), having a formal charge 2+ over the whole x range. The approach of the d_{z^2}-sub-band to its full occupancy may induce structural transformations as was observed, for instance, for Ga_xNbSe_2 and Ga_xTaSe_2 systems the structures of which transformed to the spinel structure at $x = 0.12$ (Ref. 80). Depending on the M_xTX_2 phase composition, various modes of guest metals ordering are realised or the structures without long-range order in the guest layer are formed. The ordering occurs where the guest atoms' concentration exceeds a certain value, that is, where guest–guest interactions become significant. For instance, for intercalation compounds with the compositions of $M_{0.25}TX_2$ and $M_{0.33}TX_2$, the superstructures $2a \times 2a$ and $\sqrt{3} \times \sqrt{3}a$, formed due to the occupation by the guest atom of each fourth or third octahedral vacant site, respectively, are often observed (see, *e.g.*, Refs 78 and 79). In the series of related compounds $(Cr,Ni)_{0.33}TX_2$ (where T = Nb, Ta and X = S, Se) containing the atoms of two different metals in the TX_2 interlayer space, a number of structural transitions were found[81] by X-ray and neutron diffraction upon change of the Cr : Ni ratio. According to XAFS data,[82] these transitions are accompanied by a change in the ordering of the local environment of T atoms.

Layered ternary molybdenum sulfides with 3d-metals having the stoichiometry $M_{0.5}MoS_2$ were obtained by high-temperature synthesis.[83–89] Complete X-ray single-crystal investigations were performed for some of these compounds.[85,87,88] The data obtained, for instance, for $Co_{0.5}MoS_2$ (as well as for structurally similar $Fe_{0.5}MoS_2$)[85,87] demonstrate that molybdenum atoms inside the layer have a distorted octahedral environment composed of the sulfur atoms and that the closest Mo–Mo interatomic distances are not equivalent (as in 2H-MoS_2), but are broadly scattered over the range from 2.75 Å to 3.8 Å. The interlayer spacing in this compound is somewhat smaller than in 2H-MoS_2. Syntheses of other layered molybdenum sulfides were reported[90,91] (in particular, with indium and tin) with interlayer spacings virtually coinciding with that of 2H-MoS_2, although no detailed structural data for these compounds were given. It is noteworthy that interaction of a $TaReSe_4$ matrix isoelectronic to 2H-MoS_2 with indium or tin results in its intercalation, whereas interaction with 3d-metals or with gallium leads initially to disproportionation into $TaSe_2$ and $Ta_{1-y}ReSe_{4-2y}$ and then to intercalation of the phases formed.[91]

Since intercalated metals donate electrons to TX_2, systems with various types of magnetic orderings [see, for instance, Refs 61, 89, 92] as well as spin glasses[93,94] are formed with 3d-metals.

Intercalation compounds Hg_xTS_2 (T = Ti, Ta; $x = 1–1.3$) containing mercury atoms in the interlayer space[95–97] can formally be assigned to the class considered owing to their compositions. In contrast to other chalcogenides with the composition M_xTX_2, these compounds are formed even at 20 °C. In the interlayer space, mercury atoms form chains or closely packed hexagonal sheets[97] with a 'thickness' close to the atomic radius of Hg(0). Guest-to-host charge transfer is small in these compounds and amounts to 0.2 $\bar{e}$ per Hg atom in $HgTiS_2$.[96] It is of note that 2H-MoS_2 does not react with mercury, whereas a metastable phase of molybdenum disulfide obtained from $LiMoS_2$ by lithium deintercalation (presumably, 1T modification) does react. The formation of the chains and closely packed hexagonal sheets stabilised by partial charge transfer is probably the characteristic property of mercury. This feature is inherent in related layered compounds of graphite $KHgC_4$ (Ref. 98) and in crystalline complexes of low-valent mercury with a hexafluorometallate anion Hg_3MF_6, (M = Nb, Ta).[99]

IV. Single-layer dispersions of metal dichalcogenides

The exfoliation of crystalline TX_2 intercalation compounds in a solvent under certain conditions, which gives highly dispersed systems containing X–T–X single layers, was first observed for the case of TaS_2 intercalated with hydrogen. The H_xTaS_2 phase was prepared by electrolysis of a sulfuric acid solution using tantalum disulfide as a cathode.[36] Hydration of the compound obtained with a large excess of water led to the formation of opalescent dark-brown solutions stable for ~ 1 h.[69] X-Ray studies of these solutions and of solutions of NbS_2 formed under similar conditions have shown that the interlayer ordering is absent in these systems.[69]

The formation of dark-blue colloid solutions was also observed upon solvation of the intercalation compound Na_xTiS_2 by *N*-methylformamide.[66] It was noticed that these solutions remained stable in an inert atmosphere for a long time and that the constituent single-layer species carried negative charges, which was deduced from their movement to the positive electrode in the electrophoresis.[66]

Yet another popular method of layer separation consists of the ultrasound promoted hydration of TX_2-lithium intercalation compounds. Frindt *et al.*[100] pioneered the use of this method for dispersion of $LiMoS_2$. An analogous procedure was later used to prepare dispersions from lithium intercalation compounds of TiS_2,[101] $NbSe_2$,[102] TaS_2,[103] WS_2 (Refs 104, 105) and $MoSe_2$.[106]

The structure of MoS_2 single layers in an aqueous solution has been studied in detail by various methods.[107–111] Total decomposition of a three-dimensional structure has been reliably confirmed by powder diffraction.[106–109] Such typical features of the two-dimensional diffraction as the absence of the reflections corresponding to translational periodicity along the c axis (00l lines series) as well as broadening and asymmetry of $hk0$ lines (the Warren effect[112]) were found to be characteristic of a single-layer dispersion. Based on the shape analysis of $hk0$ reflections, it was suggested[110] that T atoms in MoS_2, $MoSe_2$ and WS_2 dispersions have octahedral coordination (which was additionally confirmed in the case of molybdenum disulfide by Raman spectroscopy) instead of a trigonal prismatic coordination of the initial TX_2. Moreover, diffraction patterns of these dispersions were found to contain additional $hk0$ lines which can be assigned to a superstructure in the TX_2 layers.[106,107,109] For dispersions of the same metal dichalcogenides, significant distortions of the local environment of molybdenum and tungsten atoms, in particular, the appearance of short T–T contacts (~ 2.8–2.9 Å) corresponding to metal–metal bonds were revealed by the EXAFS technique.[106,109] Rearrangement of the energy band structure of the $(MoS_2)^{x-}$ layers in single-layer dispersions is indicated by optical

absorption spectra where no absorption maximum corresponding to a transition between valence and conduction band at 700 nm typical of the initial matrix was present.[109]

The presence of a negative charge on the layers of disulfide TS_2 dispersed in aprotic media (for instance, in the above-mentioned system Na_xTiS_2 – *N*-methylformamide) appears to be evident. As for dispersions obtained by hydration of lithium-intercalated compounds, they were originally considered as containing only neutral TX_2 layers.[100, 113, 114] However, experimental facts support the idea that dispersions prepared by the latter procedure are also ionic systems which contain macroanions $(TX_2)^{x-}$, retaining partial negative charge, solvated lithium cations and hydroxide anions.[115, 116] Actually, the interaction between water and the initial ionic compound, for instance, $Li^+(MoS_2)^-$, in which valence electrons are present on the molybdenum disulfide layers, should include two processes, *viz*., hydration of lithium cations leading to separation of the matrix layers,

$$Li^+(MoS_2)^- + H_2O \longrightarrow Li^+(H_2O)_n(MoS_2)^- \longrightarrow \quad (2)$$
$$\longrightarrow Li^+(H_2O)_n + (MoS_2)^-,$$

and redox interactions between the negatively charged $(MoS_2)^{x-}$ layers and water molecules leading to precipitation of MoS_2.

$$(MoS_2)^- \xrightarrow[-[(1-x)/2]H_2]{H_2O} (MoS_2)^{x-} + (1-x)\,OH^- \longrightarrow \quad (3)$$
$$\longrightarrow \cdots \xrightarrow[-(x/2)H_2]{H_2O} MoS_2\downarrow + OH^-.$$

Slowing down of the redox interaction (3) as the number of electrons on the layers decreases leads to retention of a partial negative charge on these layers for a long time. This appears to be the reason for the prolonged (up to 24 h) aggregative stability of aqueous dispersed systems $[Li^+ + (MoS_2)^{x-} + (1-x)\,OH^-]_{aq}$. This suggestion is supported by the fact that acceleration of crystalline MoS_2 precipitation occurs on removing the layer negative charge under the action of acid or air on the single-layer dispersion.[115, 117] In the case of acid, the process goes rapidly to completion and results in immediate precipitation of neutral molybdenum disulfide at low pH values. In the case of air, the process occurs much more slowly and includes initial precipitation of the layered compound $Li^+_{0.1}(H_2O)_y(MoS_2)^{0.1-}$ (see Ref. 115).

$$[Li^+ + (MoS_2)^{x-} + (1-x)\,OH^-]_{aq} \xrightarrow{O_2} \quad (4)$$
$$\longrightarrow Li^+_{0.1}(H_2O)_y(MoS_2)^{0.1-} \xrightarrow{O_2} MoS_2\,.$$

The composition of this compound shows directly the number of electrons remaining on the layers of the matrix at the moment of coagulation. Thus, the minimum negative charge needed to maintain stability of this dispersed system in water is close to 1 $\bar{e}$ per 10 molybdenum atoms.

V. Layered compounds obtained from single-layer dispersions

As was noted above, the intercalation of TX_2 crystals using traditional solid-state chemistry methods implies activation of the matrix by electron tranfer to its vacant band. Because of a rather broad band gap for the Group VIB metal dichalcogenides, their activation can only be achieved in reactions with strong reducing agents. Therefore, many types of heterolayered compounds based on these matrices cannot be obtained by traditional methods. In addition, such methods are of limited utility also for other dichalcogenide matrices if potential guests are not sufficiently thermally stable or their diffusion in the interlayer space of the matrix is substantially hindered, as, for instance, in the case of polymers. The use of single-layer dispersions as precursors for the preparation of intercalation compounds allows one to eliminate activation and diffusion restrictions, since the single-layers in dispersions bear negative charge and their entire 'surface' is available for absorption and chemical binding with an intercalant. That is why single-layer dispersion is most often used for both the preparation of the layered compounds based on molybdenum or tungsten disulfides and the synthesis of the nanocomposites containing polymeric molecules.

1. Compounds with organic and metal complex molecules

The formation of intercalation compounds with organic guest molecules was observed on adding water-immiscible organic solvents to aqueous single-layer dispersions of molybdenum disulfide.[118] In this case, thin films of layered compounds containing molecules of the solvent or dissolved organic compounds are formed on the interface. This method has been employed to prepare large series of intercalation compounds with benzene, styrene, hexane,[118] tetrachloroethylene,[119, 120] ferrocene [118] and its derivatives,[121] and clusters $Co_6X_8(PR_3)_6$ (X = S, Se, Te, R = Alk) [114] as the guest molecules. Unfortunately, experimental data reported in the cited publications do not allow one to make conclusions concerning the formation mechanism of the compounds obtained and, in particular, to answer the question whether the negative charge is retained on the matrix layers. Actually, according to the ionic model of the single-layer dispersion structure, the layers of metal dichalcogenides are negatively charged. If this charge rests, at least partially, in the intercalation compounds with neutral molecules listed above (what is more, most of them are not electron donors) on the matrix layers, the cations, as, for instance, Li^+ or H^+, have to be present along with these molecules. Thus the lithium cations are very likely to balance a residual negative charge of the matrix layers in the compounds $Li_{0.1}(HNR_2)_yMoS_2$,[122] which was found to be formed in the reaction of neutral dialkylamines with dispersed MoS_2.

It cannot also be excluded that macroanions $(MoS_2)^{x-}$ are completely discharged during the formation of the layered compounds. The driving force of the occlusion of neutral molecules between the non-charged matrix layers may lie in lowering the surface energy of quasi-two-dimensional layers due to the sorption of the quest molecules. The possibility of this mechanism is deduced, for instance, from the precipitation of a layered compound with naphthalene from aqueous lithium-containing MoS_2 dispersion and a solution of naphthalene in CH_2Cl_2. It was reported [123] that storage of the dispersion – organic phase system for a long time (up to 14 days) did not result in precipitate formation, but a precipitate of compound $(C_{10}H_8)_x(H_2O)_yMoS_2$ containing only traces of lithium was obtained upon acidification to pH 2. As the time of stirring increased, the *x*-value in the compounds obtained increased from 0.07 to 0.20.

Unambiguous proof of the ionic structures of aqueous MoS_2 and WS_2 dispersions was obtained in the studies of their interactions with cationic compounds. It was reported [115] that the replacement of lithium cations in the dispersions by cations less prone to hydration (*e.g*., tetraalkylammonium cations) results in virtually immediate precipitation of the layered compounds containing monolayers of the corresponding cations. These compounds contain neither water molecules as the hydration shell of the cations between the layers nor noticeable amounts of the halogen, which is consistent with the ionic mechanism of their formation.

$$(MoS_2)^{x-} + x\,R_4N^+ \longrightarrow (R_4N)_xMoS_2\,. \quad (5)$$

An analogous conclusion concerning the ionic mechanism of the reaction was made from the study [124] of the intercalation of a cationic cluster $[Al_{13}O_4(OH)_{24}(H_2O)_{12}]^{7+}$ (AL13) into MoS_2 and WS_2 matrices using their aqueous dispersions obtained by hydration of lithium-containing intercalation compounds and washed with water up to neutral pH. The same mechanism is supported by the results of intercalation of AL13, $Fe_6S_8(PEt_3)_6^{2+}$ and Cp_2Co^+ into TaS_2 using single-layer dispersions obtained by exfoliation of Na_xTaS_2 in a water – *N*-methylformamide medium.[125, 126]

As might be expected from the ionic mechanism of the reaction (5), the content of the intercalated cations in precipitated products depends on the negative charge retained on the layers at the moment of formation of a given compound as well as on the geometrical sizes of the cations (more precisely, on the minimum matrix layer area occupied by the corresponding cation). As was shown for the series of compounds $(R_4N)_xMoS_2$,[115,127] this charge can reach ~ 0.3 ē per Mo atom for the intercalation of Me_4N^+ or RMe_3N^+ cations, which form closely packed monolayers between the neighbouring MoS_2 layers. In this case, the long-chain n-alkyl substituents R in RMe_3N^+ are oriented perpendicular to the MoS_2 layers (Fig. 5). For the cations occupying a greater layer matrix area (*e.g.*, for R = Et, Pr, *etc.*), the content of the cation $x = 0.3$ cannot be achieved in a closely packed monolayer for steric reasons. Therefore, even with the excess of R_4NX salt, the charge on the MoS_2 single layers decreases in the course of formation of the compounds up to the sterically permitted value (Table 2). It can also be noted that the packing of organic cations between the layers of molybdenum disulfide depends on the content of cations in the compound and that in all cases the packing giving minimum interlayer spacing with the given guest content is realised. Thus, varying the nature and the concentration of intercalated cations, the thickness of organic layer in the compound may be changed from its minimum value of ~ 5 Å which is characteristic of all tetrasubstituted ammonium cations (and corresponds to the NC_4 tetrahedra orientation shown in Fig. 6) to ~ 29 Å for the case of n-$C_{18}H_{37}Me_3N^+$ (see Ref. 127).

Nitrogen-contaning bases may also serve as sources of cations that initiate the formation of intercalation compounds from MoS_2 single-layer dispersions. Upon protonation in aqueous solution, these bases are intercalated as mixtures of cationic species and neutral molecules. For instance, the synthesis of two types of MoS_2 intercalation compounds with 1,10-phenanthroline (phen) has been described.[128] Their structures depended on the acidity of the reaction medium. In $(phen)_{0.1}MoS_2$, the flat phenanthroline molecules are parallel to molybdenum disulfide layers ($\Delta c = 3.5$ Å), whereas, in $(phen)_{0.3}MoS_2$ ($\Delta c = 8.8-9.4$ Å), they are inclined and probably form piles (Fig. 7). Structural models proposed for compounds with phenanthroline were confirmed by EELS data obtained on the oriented particles. Calculations of the volumes occupied by the guest showed that in both cases phenanthroline molecules are closely packed in the interlayer space of MoS_2. Close packing was also observed upon MoS_2 intercalation with another compound, *viz.*, hexamethyltetraazacyclotetradecaneacetic acid. In this case, guest molecules were oriented parallel to the matrix layers.[129]

However, the examples where the space between the guest molecules is occupied by solvent molecules are also known for the intercalation compounds obtained from single-layer dispersions. In particular, this was observed for the above-mentioned co-

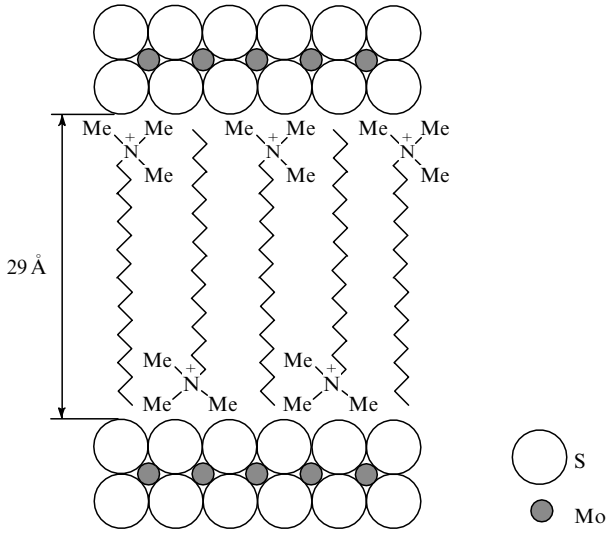


Figure 5. Orientation of intercalated tetraalkylammonium cations in the layered compound $(C_{18}H_{37}Me_3N)_{0.25}MoS_2$.[127]

Table. 2. Composition and structural parameters for intercalation compounds $(R_4N)_xMoS_2$ obtained from aqueous single-layer dispersions.[127]

Guest	Guest : host /mol mol^{-1}	Δc /Å
$(CH_3)_4N^+$	0.29	4.9
$(C_2H_5)_4N^+$	0.17	4.8
$(n\text{-}C_3H_7)_4N^+$	0.14	5.4
$(n\text{-}C_4H_9)_4N^+$	0.15	7.9
	0.12	5.2
$(n\text{-}C_6H_{13})_4N^+$	0.12	8.3
	0.05	5.0
$n\text{-}C_{12}H_{25}(CH_3)_3N^+$	0.16	8.2
	0.15	8.2
	0.08	4.8
$n\text{-}C_{14}H_{29}(CH_3)_3N^+$	0.19	12.2
	0.05	5.0
$n\text{-}C_{16}H_{33}(CH_3)_3N^+$	0.27	27.1
	0.05	4.9
$n\text{-}C_{18}H_{37}(CH_3)_3N^+$	0.25	29.2
	0.05	4.9

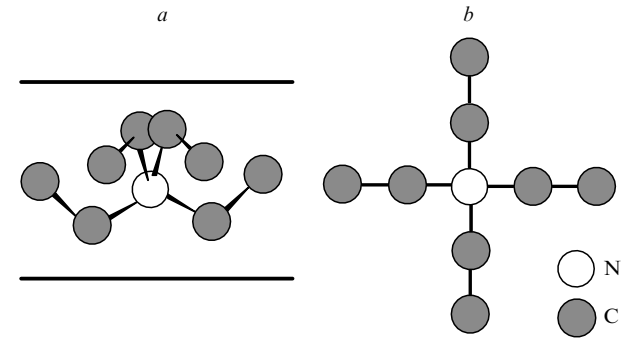


Figure 6. Orientation of Et_4N^+ cations with respect to the matrix layer corresponding to the minimum guest layer thickness.[127]
Projections onto the *ac* (*a*) and *ab* (*b*) planes.

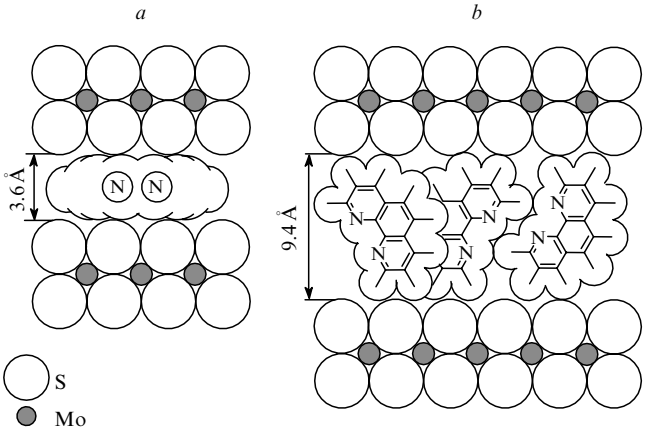


Figure 7. Schematic representation of the structures of two types of MoS_2 intercalation compounds with phenanthroline.[128]
(*a*) $(phen)_{0.1}MoS_2$, (*b*) $(phen)_{0.35}MoS_2$.

intercalation of naphthalene and water into MoS_2.[123] In the case of MoS_2 intercalation with polyoxoanions AL13, their content (0.04 mol per mol MoS_2) was lower than the maximum allowed for a closely packed monolayer (0.06 mol per mol MoS_2) and up to 20 water molecules per cluster was contained in the interlayer space.[124] In the compound $[Fe_6S_8(PEt_3)_3]_{0.05}TaS_2$, there are up to 40 molecules of H_2O or *N*-methylformamide for each intercalated cation (according to the elemental and thermogravimetric analyses data).[126]

It is worth noting that single-layer dispersions were found to be a rather convenient 'tool' for the intercalation of cationic complexes. In addition to the above-mentioned examples, preparation of the MoS_2 intercalation compounds with cationic tris(phenanthroline)- and tris(bipyridine)–3d-metal comlexes,[130] the Fe(III) complex with porphyrin[131] as well as with the ruthenium–arene aqua complexes[132] may also be noted.

In a number of examples, intercalation of complexes at room temparature is accompanied by their chemical transformations. For instance, the elimination of three phosphine ligands occurred in the formation of the layered compounds from cobalt phosphine chalcogenide clusters $Co_6X_8(PR_3)_6^{2+}$ (Refs 114, 133) and their iron-containing analogue $Fe_6S_8(PEt_3)_6^{2+}$ (Ref. 125). The intercalated layer thickness in the layered systems formed varied from 9.5 to 15.3 Å depending on the structural features of the ligands. It is thought that the liberated coordination sites around the metal atom were initially occupied by solvent molecules and not by the sulfur of the TX_2 layers. This follows from the orientation of the complexes in the interlayer space [with the C_3 axis of the Fe_6 octahedron perpendicular to the layers (Fig. 8 *a*)] proposed on the basis of the X-ray diffraction study of the electron density distribution along the *c* axis in compound $[Fe_6S_8(PEt_3)_3]_{0.05}TaS_2$ (Δc = 11.5 Å).[125, 126] Heating at 200 °C (Refs 114, 126) as well as the action of the electron beam in the electron microscope[133] results in the removal of residual phosphine ligands and in the decrease in the intercalated layer thickness up to 6–8 Å. Based on these facts, it was suggested that the species with composition Co_6X_8 or Fe_6S_8 remain in the interlayer space. Note that such clusters are most likely chemically bound to the sulfur atoms of the matrix layers.

Interaction of an MoS_2 single-layer dispersion with ruthenium–arene aqua complexes $[(arene)Ru(H_2O)_3]^{2+}$ may also be accompanied by their chemical transformations. It was shown[132] that, depending on the pH of the reaction media, the complexes are intercalated in a monomeric form (weakly acidic medium) or in the form of dimeric complexes $[(arene)Ru(\mu\text{-}OH)_3Ru(arene)]^+$ produced *in situ* due to condensation if the reaction is carried out in a weakly basic medium. Interatomic Ru–C, Ru–O and Ru···Ru distances in the intercalated complexes found by EXAFS for the benzene derivative corresponded to the distances in the known dimeric complex $[(C_6H_6)Ru(\mu\text{-}OH)_3Ru(C_6H_6)]^+$. Interlayer spacings and compositions observed for intercalation compounds with binuclear complexes $[(arene)Ru(\mu\text{-}OH)_3Ru(arene)]^+$ depended on the substituents in the ligands and were found to be 6.0 Å (x = 0.12), 10.6 Å (x = 0.11), and 5.8 Å (x = 0.06) for benzene, 1,2,4,5-tetramethylbenzene and 1-methyl-4-isopropylbenzene derivatives. These data agree well with the structural model in which arene ligands are oriented perpendicular to the matrix layers (Fig. 8 *b*) and the complexes completely fill the interlayer space.[132]

Filling of the interlayer space of molybdenum disulfide by tris-phenanthroline- and tris(bipyridine)–metal complexes $M(chel)_3^{2+}$ (M = Fe, Co, Ni, chel = 2,2′-bypyridine, 1,10-phenanthroline) in their reactions with an aqueous MoS_2 single-layer dispersion is accompanied by partial dissociation of these complexes.[130] It is evidenced by the presence of metal oxides (hydroxides) in the reaction products found by Mössbauer spectroscopy for iron complexes as examples. The oxide compounds present as an admixture are removed by treatment with acid. Mössbauer parameters of the complexes remaining in the interlayer space conform to those of their low-spin crystalline analogues and suggest somewhat greater distortions in ligand surrounding of the metal in the intercalated cationic complexes.[130] Interlayer spacings in $[M(chel)_3]_xMoS_2$ (x = 0.02–0.03) with phenanthroline (8 Å) and bipyridine (8.5 Å) ligands are consistent with the orientation of the C_3 axis of the corresponding complexes perpendicular to the layers (Fig 8 c).

It was also reported[134] that MoS_2 is intercalated with alkali metal complexes of crown ethers (12-crown-4, 15-crown-5 and 18-crown-6). However, the obtained layered compounds were unstable and washing with water resulted in the extraction of the intercalant.

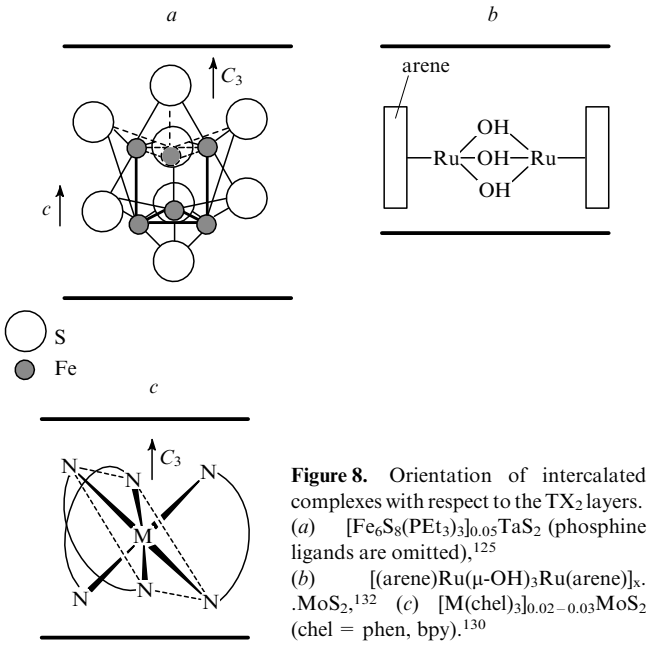


Figure 8. Orientation of intercalated complexes with respect to the TX_2 layers. (*a*) $[Fe_6S_8(PEt_3)_3]_{0.05}TaS_2$ (phosphine ligands are omitted),[125] (*b*) $[(arene)Ru(\mu\text{-}OH)_3Ru(arene)]_x$. MoS_2,[132] (*c*) $[M(chel)_3]_{0.02-0.03}MoS_2$ (chel = phen, bpy).[130]

2. Nanocomposites with polymers

A wide range of compounds in which the interlayer space of TX_2 is filled with polymeric molecules are currently known.[101–103, 134–148] Such compounds, which consist of two extended structures differing in chemical nature, belong to nanocomposite materials. Experimental data for nanocomposite materials based on TX_2 and polymers are given in Table 3. It should be mentioned that synthesis of polymer–inorganic matrix hybrid composite materials is now taking features of the whole line of inquiry which continues to grow in popularity (*e.g.*, see Ref. 149). Such nanocomposites based on metal dichalcogenides are mostly obtained by adding aqueous solutions of a polymer to aqueous TX_2 single-layer dispersions. Sometimes, other solvents are also used as, for instance, *N*-methylpyrrolidinone for PANI,[135] CF_3CH_2OH for Nylon-6 and decalin for polyethylene.[138] In this case, the formation of nanocomposites can proceed in a water–organic solvent biphasic system. For pyrrole[147] and styrene,[148] *in situ* polymerisation was carried out. Pyrrole was introduced in an aqueous dispersion as a monomer along with $FeCl_3$, and macromolecules formed upon its oxidative polymerisation filled the space between the molybdenum disulfide layers. Polymerisation of styrene is believed to occur in the interlayer space.[148] An interesting modification of a procedure for the preparation of these materials is a layer-by-layer deposition of the MoS_2 layers from dispersions and the layers of a polymer from its solution in poly(allylamine hydrochloride).[143] It was noted[143] that, independent of the absorption time, the increase in the film thickness in each cycle corresponded to one monolayer in agreement with a growth mechanism based on the mutual compensation of the charges of polyanions of single-layer $(MoS_2)^{x-}$ and the polycationic polymer.

Table 3. Nanocomposite materials based on TX_2 and polymers.

Composition [a]	Δc /Å	σ /Ω^{-1} cm^{-1}	Ref.
Poly(ethylene oxide) as the polymer			
$(PEO)_{1.0}MoS_2$	8.35	0.02	136, 138
$(PEO)_{0.92}MoS_2$ (see [b])	10.1	0.10	136, 138
$Li_{0.12}(PEO)_{1.34}MoS_2$	8.4	–	139
$Li_{0.1}(PEO)_{1.0\text{-}1.3}MoS_2$	8.0	–	101
$Li_{0.1}(PEO)_{0.5}MoS_2$	5.4	0.0005	145
$Li_{0.1}(PEO)_{1.0}MoS_2$	10.2	0.0066	145
$Li_{0.09}(PEO)_{1.28}MoS_2$	8.2	–	144
$Li_{0.21}(PEO)_{1.6}MoS_2$	10.0	0.061	134
$Na_{0.13}(PEO)_{0.8}MoS_2$	6.4	0.0011	134
$K_{0.22}(PEO)_{0.3}MoS_2$	3.3	0.047	134
$Rb_{0.17}(PEO)_{0.6}MoS_2$	3.5	0.084	134
$Cs_{0.45}(PEO)_{1.0}MoS_2$	10.0	0.0004	134
$K_{0.1}(PEO)_{0.5}MoS_2$	4.8	–	140
$K_{0.1}(PEO)_{1.2}MoS_2$	9.0	–	140
$M_{0.3}(PEO)_{0.8}TiS_2$ (M = Li, Na)	8.2	–	101
$Li_{0.15}(PEO)_{1.14}(H_2O)_{0.56}(PbS)_{1.18}(TiS_2)_2$	8.5	–	146
$Li_{0.25}(PEO)_{1.79}(H_2O)_{0.88}\ (PbS)_{1.18}(TiS_2)_2$	8.4	–	146
$Li_x(PEO)_yMoSe_2$	7.9	–	101
$(PEO)_{0.94}NbSe_2$	13.3	250	102
$(PEO)_{0.80}NbSe_2$ [b]	12.5	240	102
$Li_{0.2}(PEO)_{1.36}TaS_2$	9.6	19	103
$Li_{0.2}(PEO)_{1.68}TaS_2$	9.5	3.0	103
$Li_{0.2}(PEO)_{1.51}(H_2O)_{0.23}TaS_2$	9.2	2.2	103
$Li_{0.2}(PEO)_{0.75}(H_2O)_{0.06}TaS_2$	9.1	17	103
Poly(propylene glycol) as the polymer			
$(PPG)_{0.5}MoS_2$	8.25	0.20	136, 138
Poly(vinylpyrrolidone) as the polymer			
$(PVP)_{0.76}MoS_2$	14.95	0.003	136, 138
$(PVP)_{0.14}NbSe_2$	17.7	140	102
$Li_{0.2}(PVP)_{0.95}TaS_2$	25.1	31	103
$Li_{0.2}(PVP)_{1.28}(H_2O)_{0.35}TaS_2$	24.7	0.5	103
Methylcellulose as the polymer			
$(MCel)_{0.26}MoS_2$	14.25	0.0004	136, 138
Poly(ethylene imine) as the polymer			
$(PEI)_{0.83}MoS_2$	4.05	0.005	136, 138
$Li_x(PEI)_{0.82}TaS_2$	4.0	125	103
$Li_x(PEI)_{3.2}(H_2O)_{0.56}TaS_2$	30.8	0.18	103
Nylon-6 as the polymer			
$(Nylon\text{-}6)_{3.6}MoS_2$	11.35	$<10^{-6}$	136, 138
Polyethylene as the polymer			
$[(CH_2)_n]_3MoS_2$	4.15	$<10^{-6}$	136, 138
Polyaniline as the polymer			
$(PANI)_{0.35}MoS_2$	10.4	0.4	135, 136
Polypyrrole as the polymer			
$(PPY)_{0.24}MoS_2$	4.5	–	147
Poly(allylamine) as the polymer			
see [c]	8.65	–	143

Note. The following notations are used: PEO, poly(ethylene oxide); PPG, poly(propylene glycol); PVP, poly(vinylpyrrolidone); MCel, methylcellulose; PEI, poly(ethylene imine); PANI, polyaniline, PPY, polypyrrole.

[a] The composition displays the content of monomer units per TX_2 formula unit. [b] Low-molecular polymer with $M_w < 10\,000$ is used. [c] Film obtained by layer-by-layer deposition of polymer and MoS_2.

Most polymer-containing nanocomposites were obtained with the use of molybdenum disulfide single-layer dispersions (see Table 3). The same approach was also used for other dichalcogenide matrices which can form dispersions, such as, $NbSe_2$,[102] TaS_2,[103] TiS_2 (Ref. 101) and $MoSe_2$.[101]. A misfit compound $(PbS)_{1.18}(TiS_2)_2$ has also been used as a matrix in the synthesis of nanocomposites with polymers.[146] In the structure of this compound, uncommensurate layers [150] alternate in the sequence S–Ti–S···S–Ti–S···PbS. Synthesis of the nanocomposite was carried out by intercalation of lithium folowed by the exfoliation performed directly in an aqueous PEO solution. The data from X-ray and electron diffraction analysis [146] are consistent with the viewpoint that the polymer molecules fill the van der Waals gaps only between the adjacent TiS_2 layers.

It was noted for many examples, that alkali metal cations enter into the interlayer space (0.1–0.2 atom per T atom) along with a polymer.[101, 103, 139, 140, 144, 145] This agrees with the retention of the charge separation between the guest and the host in these intercalation compounds as in the case of compounds with molecular guests.

The cations situated in the interlayer space of metal dichalcogenides may form complexes with polymers. This is particularly characteristic of PEO. Based on the analysis of ^{23}Na NMR spectra, it has previously been noted that strong cation–polymer interactions take place in related systems with aluminosilicates.[151] Similar conclusion has been made from the study of ^{7}Li NMR spectra and electron density distribution in $Li_x(PEO)_yMoS_2$ phases [103] as well as from the data from IR spectroscopy obtained for $Li_x(PEO)_y(PbS)_{1.18}(TiS_2)_2$.[146] Complexing properties of poly(ethylene oxide) with respect to alkali metals have been specially used for the preparation of the nanocomposites with MoS_2.[134] Precipitation was carried out from aqueous solutions of PEO and ACl (A is an alkali metal). The nanocomposites obtained contained no chlorine and relative amounts of A and PEO depended on the nature of the alkali metal. Thicknesses of the polymer-containing layers also depend on the nature of the metal and vary in the reaction products from 3.3 to $\sim$ 10 Å (see Table 3). This is apparently due to the difference in geometry of the complexes formed by the metal with the polymer units.

^{13}C NMR studies of the conformation of poly(ethylene oxide) in the nanocomposite $Li_{0.09}(PEO)_{1.28}MoS_2$ do not give an unambiguous answer to the question about the polymer packing. It was found that $\sim$ 90% of the O–C–C–O fragments of the polymer chain are in the *gauche* conformation, whereas, according to the calculations, the content of such fragments in stretched polymer molecules inscribed into the tunnels of 8 Å diameter should be 50% and 100% upon chaotic and spiral packings, respectively (in the latter case, all the *gauche* conformers are of the same sign).[144] It should be mentioned that spiral packing is characteristic of PEO–ACl complexes.[152] Yet another model accounting for possible solvation of lithium cations by oxygen atoms of the polymer is that polymer units form flat rings resembling crown ethers, with the oxygen atoms being directed inward. In this case, the content of O–C–C–O fragments in *gauche* conformations (with the alternating signs) may amount to 75%. This percentage may be exceeded which requires that the conformational equilibrium of C–O–C–C chain fragments are shifted from *trans* to *gauche* conformers.

As was pointed out in many publications dealing with nanocomposites of molybdenum disulfide and polymers, the electrical

conductivity (σ) of the nanocomposites markedly increases with respect to that of MoS_2; σ values were found to be $\sim 6\times10^{-6}$ (Ref. 134) or 2×10^{-7} Ω^{-1} cm^{-1} (Ref. 145). Despite the differences in the σ values (*cf.* Table 3, compounds with PEO), this increase has been well established for the nanocomposites with both conducting (*e.g.*, PANI) and non-conducting (*e.g.*, PEO) polymers. The exception is provided by the compounds with nylon and polyethylene for which no increase in conductivity was observed. The fact that electrical conductivity of nanocomposites slightly increases with temperature and that these materials exhibit Pauli paramagnetism at 50–300 K [136, 138] allow one to attribute them to semimetals. The increase in electronic conductivity in the nanocomposites based on MoS_2 is usually associated with a structural rearrangement of the layers of the initial MoS_2 (and a corresponding change in the type of its electronic structure) from 2H (semiconductor) to 1T (semimetal) modification during the dispersion process. In some cases, the conductivity of the compounds was found to decrease gradually on ageing or on heating at 100–200 °C. This is interpreted as a gradual structural reverse transition 1T → 2H which has earlier been observed [31] for pure 1T-MoS_2. However, it should be noted that the 1T modification is apparently stabilised in the presence of a polymeric guest or/and the charge on the matrix layers. This is deduced from the fact that the transition to the 2H-structure manifested as an exothermic effect in the curves of differential thermal analysis occurs at higher temperatures (up to 177 °C) for the nanocomposites than for pure 1T-MoS_2 (94 °C).[138]

Conductivity is noticeably higher for polymer-containing nanocomposites based on the Group VB metal dichalcogenides than for their analogues based on MoS_2. However, conductivity of the former is lower than that of the corresponding non-intercalated TX_2, as could be expected from band structure considerations.

The nanocomposites considered also possess ionic conductivity (σ_i) along with electronic conductivity (σ_e). It was shown [145] that the ionic conductivity of $Li_{0.1}(PEO)_1MoS_2$ is $\sim 10^{-6}$ Ω^{-1} cm^{-1}, while σ_e/σ_i is 10^3. The ionic conductivity of this compound is obviously caused by the mobility of lithium ions which is significantly higher in the nanocomposites than in Li_xMoS_2. For instance, at 25 °C the diffusion coefficient of lithium in $Li_{0.1}MoS_2$ equals 4×10^{-13} cm^2 s^{-1}, whereas it reaches 5×10^{-12} and 10^{-10} cm^2 s^{-1} in $Li_{0.1}(PEO)_1MoS_2$ and $Li_{0.1}(PEO)_{0.5}MoS_2$, respectively.[145]

At a temperature of 14–15 K, a metal–insulator transition is observed for MoS_2-based nanocomposites,[138] while $NbSe_2$- and TaS_2-based compounds exhibit superconductivity at cryogenic temperatures.[102, 103] The highest temperature of the transition to the superconducting state, $T_c = 7.1$ K, which is virtually equal to T_c for a non-intercalated matrix [7.2 K (see Ref. 3)] was found for $(PVP)_{0.14}NbSe_2$.[102] In the cases of TaS_2 nanocomposites with PEO, PVP and PEI, an increase in T_c (up to 2.5–2.9 K) as compared with T_c of the initial 2H-TaS_2 (0.8 K) was observed.[103]

3. Compounds with metals and metal hydroxides

The formation of precipitates upon addition of metal salts to single-layer dispersions has been observed in the earliest publications describing the behaviour of dispersed TX_2. Thus Lerf and Schöllhorn [66] pointed to the precipitation of compounds with non-established structures upon action of lanthanum salts on TiS_2 dispersion in *N*-methylformamide. The precipitation of powdered compounds upon action of salts of various metals (Al, In, Ni, Co, Ce, Sr, Cd, Zr, Zn, Pb) on single-layer dispersions was observed by Gee *et al.*[153] In the authors' opinion, these were the 'inclusion compounds' containing metal hydroxides distributed throughout the MoS_2 matrix.

However, more recent studies on the reactivity of molybdenum disulfide dispersed in water showed that the compounds formed may differ in their nature, the latter being determined by both the nature of metal cations involved in the interaction and the reaction conditions. If the alkali metal cations are present in solution, the corresponding layered solvates $A_x(H_2O)_yMoS_2$ (A = Li, $x = 0.12$; A = K, $x = 0.2$) are precipitated from single-layer dispersions, the same solvates are also formed in the exchange of intercalated organic cations with cations A^+ (see Ref. 115). In the presence of metal (M) cations able to form coordination bonds with sulfur atoms of the MoS_2 layers, two reaction pathways are possible. One of them leads to the formation of compounds similar to the above-described ternary molybdenum sulfides M_xMoS_2, the other leads to the filling of the interlayer space with metal hydroxo compounds (Eqns 6a, 6b).

$$[Li^+ + (MoS_2)^{z-} + (1-x)\,OH^-]_{aq} \xrightarrow{M^{n+},\ H_2O}$$

$$\rightarrow M_xMoS_2 \qquad (6a)$$

$$\rightarrow M_y(OH)_{ny-x}(H_2O)_xMoS_2 \qquad (6b)$$

Obviously, the type of the compound formed is determined by the tendency of metal cations to form sulfide derivatives with MoS_2 or oxo(hydroxo) compounds in an aqueous medium. Thermodynamic characteristics of sulfide macroanions $(MoS_2)^{x-}$, in particular the stability constants of their complexes are not known, while the characteristics of binary sulfides are well known. Therefore, for a large series of metals, the compositions of intercalation compounds formed were correlated with the difference in solubility products (pK_{sp}) of the corresponding metal sulfides MS_y and hydroxides $M(OH)_n$.[154] It was noted that, if K_{sp}[MS] and K_{sp}[M(OH)$_2$] differ by 2–4 orders of magnitude (Mn^{2+}, Fe^{2+}, Co^{2+}, Ni^{2+}), compounds with alternating S–Mo–S and hydroxide-like $M(OH^-)_{2-x}(H_2O)_x^{x+}$ layers are formed [see Eqn (6b)]. The cations characterised by $K_{sp}[MS]-K_{sp}[M(OH)_2] \simeq 10^{11}-10^{14}$ (Pb^{2+}, Cd^{2+}) exhibit a strong tendency to form coordination bonds with sulfur atoms of MoS_2, but can yet be intercalated in the form of hydroxo compounds upon increase in pH. It is only in the case where the difference mentioned exceeds 16 orders of magnitude that the formation of ternary sulfides (6a) dominates in single-layer dispersions.

a. Phases intercalated with hydroxo compounds

Upon precipitation of aqueous MoS_2 single-layer dispersions in the presence of hydrated rare-earth [La^{3+}, Er^{3+}, Th^{4+} (see Ref. 155)] or 3d-metal cations, aqua(hydroxo) compounds fill the interlayer space.[153, 155] Freshly precipitated compounds with rare-earth elements possess distinct layered structures and are characterised by a large increase in the interlayer distance (for instance, in the case of Er^{3+}, Δc value reaches 9.8 Å). However, amorphisation of these compounds occurs in a few hours. This may be explained by the tendency of intercalated cations to form compounds with a high (up to 8–12) and variable content of water molecules in the hydration shell and it is the loss of these molecules on ageing that causes amorphisation.

The parameters of layered MoS_2 compounds with 3d-metals remain invariable at room temperature for a long time. For the substances formed in the interlayer spaces of these compounds, both the composition (atomic M : O ratio determined by EELS [116]) and the local structure [interatomic M–O and M···M distances determined by EXAFS for the compounds with Mn, Co, Ni (see Refs 64, 156–158)] are close to those of the corresponding metal hydroxides $M(OH)_2$. These hydroxides themselves are known to have a layered hexagonal structure in which the metal atoms occupy the octahedral sites between two closely packed layers of the hydroxide ions (which corresponds to the polytype 1T in the classification of transition metal dichalcogenides).[159] For some crystalline 3d-metal (Mn, Fe, Co, Ni) hydroxides, the parameters a of their hexagonal lattices, defining the M···M and anion–anion distances inside the layer, are close to those of MoS_2, the deviation being in the range of a few percents (Table 4). Commensurability of the lattices of two substances

Table 4. Structural parameters (Å) of intercalation compounds $[M(OH)_2]_{1/2}MoS_2$ and the corresponding metal dihydroxides $M(OH)_2$ determined by powder diffraction and EXAFS.[158]

M	$[M(OH)_2]_{1/2}MoS_2$				$M(OH)_2$		
	c	Δc	r_{M-O}	$r_{M\cdots M}$	c	r_{M-O}	$r_{M\cdots M}$
Mn	11.3	5.1	2.20	3.29	4.68	2.23	3.33
Co	11.3	5.1	2.08	3.15	4.64	2.10	3.18
Ni	11.5	5.3	2.06	3.11	4.60	2.07	3.14

different in nature obviously favours the formation of the structure with alternating metal sulfide and metal hydroxide layers (Fig. 9) in a single-layer dispersion.

$$[Li^+ + (MoS_2)^{x-} + (1-x)\,OH^-]_{aq} \xrightarrow{M^{2+}} \quad (7)$$

$$\longrightarrow [M_{0.5}(OH)_{1-x}(H_2O)_x]^{x+}(MoS_2)^{x-} \longrightarrow$$

$$\xrightarrow{O_2} M^{II}_{0.5-x}M^{III}_x(OH)MoS_2 + (x/2)\,H_2O \quad (7a)$$

$$\longrightarrow M_{0.5}(OH)MoS_2 + (x/2)\,H_2 \quad (7b)$$

Presumably, in the formation of compounds with 3d-metals, the extended two-dimensional aqua-hydroxo-clusters $[M_{0.5}(OH)_{1-x}(H_2O)_x]^{x+}(MoS_2)^x$, which compensate the negative charge of the disulfide monolayer, are initially produced on the surface of $(MoS_2)^{x-}$ single layers [Eqn (7)]. During precipitation and ageing, the structure of these intercalated clusters is transformed into a thermodynamically more stable structure of pure metal hydroxide through replacement of water molecules by OH^- anions. Such a transformation can occur upon oxidation of part of the ions M(II) in the guest layer by oxygen leading to a mixed hydroxide M(II,III)$(OH)_2$ [reaction (7a)] and also upon reduction of water molecules with evolution of molecular hydrogen [reaction (7b)].[130]

It is obvious that the reaction (7a) is favoured by the ability of metal ions to adopt a higher oxidation state. It has been shown by means of ^{57}Fe Mössbauer spectroscopy and electron microscopy that the reaction of single-layer dispersion with $Fe(II)_{aq}$ follows this pathway and that the product contains Fe(II) and Fe(III) in the oxygen environment.[116] Temperature dependence of the Mössbauer spectra of the iron-containing compound indicates that magnetic ordering occurs simultaneously for both iron forms in a narrow temperature range ($\sim$ 10 K). This suggests the presence of both these forms in a single structure. The character of the transition points to a small size of magnetic domains and their narrow size distribution. The formation of a joint structure by both forms of iron is also deduced from the occurrence of a thermally activated fast electronic exchange between them, which results in the appearance of an iron state with intermediate Mössbauer parameters at 300–380 K.[160, 161]

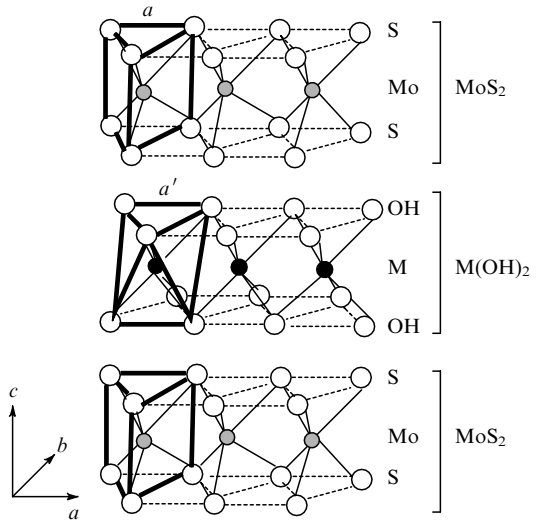


Figure 9. Alternating monolayers of MoS_2 and $M(OH)_2$ in the layered compound.

The reaction pathway (7b) is realised in the case of compounds with Co(II) and Ni(II). Measurements of magnetic characteristics of the precipitated products point to the occurrence of both the Co^{2+} (μ = 5.2 μ_B) and Ni^{2+} (μ = 3.2 μ_B) ions in the octahedral environment characteristic of the corresponding metal hydroxides,[162] while the interatomic distances in the intercalated layer are consistent with those in $M(OH)_2$ as was mentioned above. Complete substitution of OH^- for H_2O probably takes a long time, so the MoS_2 layer in the intercalation compounds continues to bear partial negative charge. This agrees with the prolonged conservation of characteristic distortions in the matrix layer (the set of non-equivalent Mo–Mo distances [64, 157, 158] and a superstructure in the plane of the layers [163]) in these compounds.

b. Phases intercalated with metals

Compounds with the composition M_xMoS_2 (M = Cu, Ag, Cd, Hg, Pd, Pb) formed where the $(MoS_2)^{x-}$ layers act as polysulfide macroligands were obtained by precipitation of single-layer dispersions in the presence of the cations noted.[154, 164–166] Judging from the M–S distances, the intercalated metal atoms form direct covalent or ionic–covalent bonds with sulfur atoms of the matrix layers (EXAFS data [154, 165, 166]). It is of note that there are no direct analogues to the above-mentioned compounds among the known ternary molybdenum sulfides obtained by high-temperature synthesis where the S–Mo–S layers are only present in the structures of compounds with 3d-metals [V, Cr, Fe, Co (see Refs 83–89)]; the other metals [*e.g.*, Ga and Al (see Ref. 167)] form compounds with a spinel structure.

In the dispersions, the charged molybdenum disulfide single-layers exhibit reducing properties with respect to the cations characterised by the positive redox potentials.[154] For instance, for Ag^{2+}, Pd^{2+} and Hg^{2+}, their reduction products [Ag(0), Pd(0), Hg_2^{2+}] were obtained along with the M_xMoS_2 phases.[154, 165, 166] In the case of Cu^{2+}, the reduced Cu^+ cations were incorporated into the layered compound formed. Hence, all the copper atoms in the prepared $Cu_{0.35}MoS_2$ had the oxidation state +1.[165] Experimental data show that the single-layers $(MoS_2)^{x-}$ reduce metal cations if the layer charge x exceeds some threshold value. The maximum layer charge equal to 1 $\bar{e}$ per Mo atom in $LiMoS_2$ decreases during the dispersion (which is accompanied by hydrogen evolution) and subsequent ageing, thus lowering the reducing ability of the $(MoS_2)^{x-}$ layers. The composition of compound $Cu^I_{0.35}MoS_2$ formed upon the action of Cu^{2+} ions on the MoS_2 single-layer dispersion indicates that this charge can reach $\sim$ 0.7 $\bar{e}$ per Mo atom in the freshly prepared dispersions and that the single-layer no longer reduces Cu^{2+} when the charge decreases to $\sim$ 0.35 $\bar{e}$ per Mo atom (see Ref. 165).

Structural parameters for the M_xMoS_2 phases are given in Table 5. It is clear from the Table that the increase in the interlayer spacing is small for various metal atoms introduced into the MoS_2 matrix, but it increases with the increase in the sizes of the guest cations. It is of note that a comparison of either Δc for this compound or the radii of the intercalated cations with the sizes of the interstitial vacant sites between the sulfur atoms (octahedral of $\sim$ 0.7 Å radius and tetrahedral of $\sim$ 0.4 Å radius) does not allow unambiguous determination of the type of occupied vacancies since the MoS_2 matrix itself may be essentially distorted and 'the thickness' of its layers may change. For instance, in the crystalline $Co_{0.5}MoS_2$ (prepared by high-temperature synthesis), the coordination environment of molybdenum is octahedral and the interlayer distance is 5.72 Å,[87] *i.e.*, the thickness of the S–Mo–S layers is smaller by $\sim$ 0.5 Å in this compound than in non-

Table 5. Interlayer spacings (c), interlayer spacing expansions with respect to MoS_2 (Δc) and parameters of the local environment of the guest atoms for ternary sulfides M_xMoS_2 obtained from single-layer dispersions.

Compound	c /Å	Δc /Å	Radius of the M^{n+} cation according to Shannon for the indicated coordination number (C.N.)			N_{M-S}	r_{M-S} /Å	Coordination polyhedron for M	Ref.
			r /Å	$n+$	C.N.				
$Cu_{0.35}MoS_2$	6.25	0.1	0.60	1+	4	3.1	2.29	tetrahedron	165
$Pd_{0.45}MoS_2$ (60% $Pd_{0.25}MoS_2$ + 40% Pd)	6.2	0.05	0.64	2+	4	2.6[a]	2.33	"	154
$Hg_{0.20}MoS_2$	6.3	0.15	0.69	2+	2	1.1	2.37	strongly distorted octahedron	154
$Hg_{0.02}MoS_2$	–	–	–	–	–	1.9	2.38	the same	166
$Hg_{0.32}MoS_2$	–	–	–	–	–	1.5	2.37	"	166
$Cd_{0.20}MoS_2$	6.55	0.4	0.78	2+	4	4.0	2.55	tetrahedron	154
$Ag_{0.86}MoS_2$ (95% $Ag_{0.82}MoS_2$ + 5% Ag)	7.0	0.85	1.00	1+	4	1.0[a]	2.40	strongly distorted tetrahedron	154
$Ag_{0.61}MoS_2$	–	–	–	–	–	1.6	2.43	the same	166
$Pb_{0.18}MoS_2$	7.1	0.95	1.19	2+	6	5.7	2.87	octahedron	154

[a] The N_{M-S} value as calculated for a pure phase of ternary sulfide.

intercalated 2H-MoS_2 in which the environment of molybdenum is trigonal prismatic.

EXAFS data has been used to estimate the type of coordination environment of intercalated metals.[154, 165, 166] The type of coordination of the guest atoms M with sulfur atoms is primarily determined by the preferable coordination polyhedra of M, both in TX_2 compounds with metals prepared by high-temperature synthesis and in M_xMoS_2 compounds obtained from single-layer dispersions. Thus Pb^{2+} ions occupy the octahedral vacancies while Cd^{2+}, Pd^{2+}, Cu^+ and Ag^+ ions have tetrahedral surroundings, non-distorted for cadmium and distorted to a variable degree for palladium, copper and silver. For the two last-mentioned metals, the displacement of their atoms to one of the vertices inside a tetrahedral vacancy is assumed based on both the experimental results and comparison with the structures of related sulfide compounds. The strongest distortion of coordination polyhedron in the interlayer space of M_xMoS_2 is probably characteristic of mercury compounds because the basic site occupied by mercury is strongly deformed to realise the most suitable near-linear coordination for Hg(II) with S atoms.

The Mo *K*-edge EXAFS [154, 165, 166] and, in some cases, X-ray and electron diffraction [165] data showed that the layer matrix in M_xMoS_2 sulfides obtained from single-layer dispersions is distorted owing to the formation of Mo–Mo bonds. At the same time, due to covalent guest–matrix bonding, these compounds are distinguished among the intercalation compounds prepared from single-layer dispersions by their most structural ordering. In particular, X-ray diffraction data [168] indicate that three-dimensional correlations in the layer stacking (rather than turbostratic packing) for the distances of 50–70 Å is characteristic of copper and silver compounds.

VI. Structural transformations of the chalcogenide matrices in the formation of single-layer dispersions

A study of the atomic structure of the TX_2 layers in both the dispersions and the layered materials precipitated from them is a non-trivial task because the subjects of investigation are layered nanostructured species, in many cases thermodynamically metastable, characterised by the absence of a long-range order and by a strong anisotropy of the interatomic interactions. Only scarce information can be obtained by XRPD for such compounds (even for those precipitated) since the diffraction is essentially two-dimensional in character owing to turbostratic packing and does not allow the unit cell structure to be completely determined. For this reason, structural studies of these materials require the application of a combination of instrumental and calculation methods. These were mainly carried out for materials based on molybdenum and tungsten disulfides because of their potential practical use and also owing to unusual structural transitions found in their quasi-two-dimensional layers.

The distinctions between the atomic structures of the MoS_2 (WS_2) layers present in single-layer dispersions or in the precipitated products and those of the most stable 2H-modifications have repeatedly been observed using physical methods, first of all, EXAFS, [64, 109, 154, 157, 158] and X-ray and electron diffraction.[109, 163, 165, 169] The main feature of the local order in the layered compounds formed is the redistribution of T···T distances. For MoS_2 compounds, three non-equivalent Mo···Mo distances (~ 2.8, ~ 3.2 and ~ 3.8 Å) were observed in the EXAFS spectra instead of one (3.16 Å) distance in 2H-MoS_2. The shortest Mo–Mo contact in the modified layer corresponds to the formation of a metal–metal chemical bond.

Currently, it is agreed that the Mo(W) atoms in the layered compounds prepared from the single-layer dispersions have an octahedral rather than a trigonal prismatic (as in 2H-MoS_2 and 2H-WS_2) coordination environment. Though this supposition is not experimentally verified to date, it appears to be quite probable taking into account the partial retention of the negative charge on the TS_2 layer in all the following consecutive transformations: $LiTS_2$ → dispersions → precipitated layered compound. Even the first calculations of the band structure carried out in the early 1970's showed that the octahedral coordination becomes more energetically advantageous for the molybdenum atoms upon adding of 1 $\bar{e}$ per Mo atom to the conduction band formed mainly by the 4d-orbitals of molybdenum. Thus, at least part of the atoms in the charged $(TS_2)^{x-}$ layer should be in the octahedral environment. Indirect evidence for the octahedral coordination has been reported.[57] In addition, this coordination is well established by X-ray diffraction analysis for single crystals of ternary sulfides $M_{0.5}MoS_2$ prepared by high-temperature synthesis.[83–88] As in $LiMoS_2$, the formal oxidation state of molybdenum in these layered derivatives of molybdenum disulfide remains +3. For $LiMoS_2$ and materials prepared from dispersions, all the structural models are based on the octahedral coordination of molybdenum postulated for the metastable modification 1T-MoS_2.[31]

Calculations by the extended Hückel method in the rigid band approximation showed [170] that the Fermi surface is characterised

by nesting † in the case of the layered systems with an octahedrally coordinated central atom with d^2 or d^3 electron configuration. In such systems, the metal atom sublattices are unstable, they undergo distortions to form charge density waves (CDW) unriging this symmetry. In same sence, CDW formation is analogous to the Jahn–Teller distortions in molecular systems,[171] while the splitting of the partially filled degenerate orbitals leading to lowering of the overall energy of the system may serve as an analogue of the splitting of partially filled d-sub-band of the metal atom causing the appearance of an energy gap between the filled valence band and the conduction band in the case of infinite quasi-two-dimensional layers. The most probable result of the distortions is the formation of triangular clusters or infinite zigzag chains built of metal atoms.[13, 170, 171]

The calculations of the $LiMoS_2$ structure with optimisation of the geometry by DFT FLAPW (Density Functional Theory, Full-Potential Linearised Augmented Plane Wave) method showed [172] that the formation of a $2a \times 2a$ superstructure (zigzag chains formed by rhombus-shaped clusters of molybdenum atoms) lowers the energy of the system. The results obtained, namely, the lengths of the contracted and elongated (with respect to the lengths in the initial 2H-MoS_2) Mo–Mo bonds in the optimised $LiMoS_2$ structure are consistent with the EXAFS results obtained at the Mo *K*-edge.[39] The same type of ordering is present in the structure of $LiMoS_2$, which was simulated based on the analysis of PDF obtained from X-ray diffraction data (Fig. 10 *a*).[65] According to this model, the structure as a whole is characterised by a triclinic symmetry ($a = 6.963$ Å, $b = 6.386$ Å, $c = 6.25$ Å, $\alpha = 88.60°$, $\beta = 89.07°$, $\gamma = 120.06°$; the space group $P\bar{1}$).

According to the data from X-ray single crystal analysis, the clusters consisting of molybdenum atoms are also present in the molybdenum ternary sulfides obtained by high-temperature synthesis.[87] For instance, the zigzag chains with direct Mo–Mo bonds exist in the $Co_{0.5}MoS_2$ structure, which contains four symmetrically independent molybdenum atoms in the unit cell (Fig. 10 *b*). Taking into account the layer stacking, the crystal lattice of $Co_{0.5}MoS_2$ belongs to a face-centered monoclinic syngony (the space group Cc, $Z = 4$, $a = 11.793$, $b = 6.548$, $c = 12.680$ Å; $\beta = 115.5°$) and the relationships between its parameters and the parameters of 2H-MoS_2 (a_0, c_0) are as follows: $a \approx 2\sqrt{3}a_0$ and $b \approx 2a_0$, $c \sin\beta \approx c_0$. Thus, the displacements of the molybdenum atoms in $Co_{0.5}MoS_2$ with respect to their positions in the 2H-MoS_2 layer can also be approximated with a $2a \times 2a$ superstructure.

† The regions of the Fermi surface coinciding with each other upon parallel transfer of the electron quasi-pulses in space.

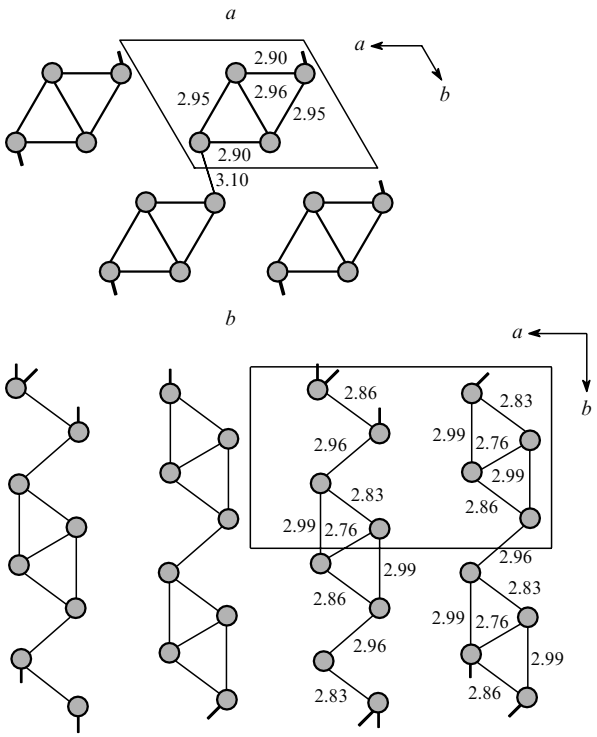


Figure 10. Schematic representation of the chains formed by molybdenum atoms in the *ab* plane in $LiMoS_2$ (*a*) [65] and $Co_{0.5}MoS_2$ (*b*).[87] Figures indicate (in Å) the values of interatomic distances contracted as compared with 2H-MoS_2.

From EXAFS and X-ray diffraction studies carried out on the single-layer dispersions themselves, it was suggested that the molybdenum atoms in the single layers are displaced from their positions in the hexagonal $a \times a$ structure and form rhombuses (Fig. 11 *a*, *b*). This should result in two Mo–Mo distances (2.8 and 3.8 Å) and multiplication of the in-layer parameters of the unit cell to $2a \times 2a$.[107, 109] Such a model fits the experimental data best of all provided the molybdenum atoms are displaced by 0.45 Å along the *a*-axis of the unit cell ($a = 3.27$ Å). Redistrib-

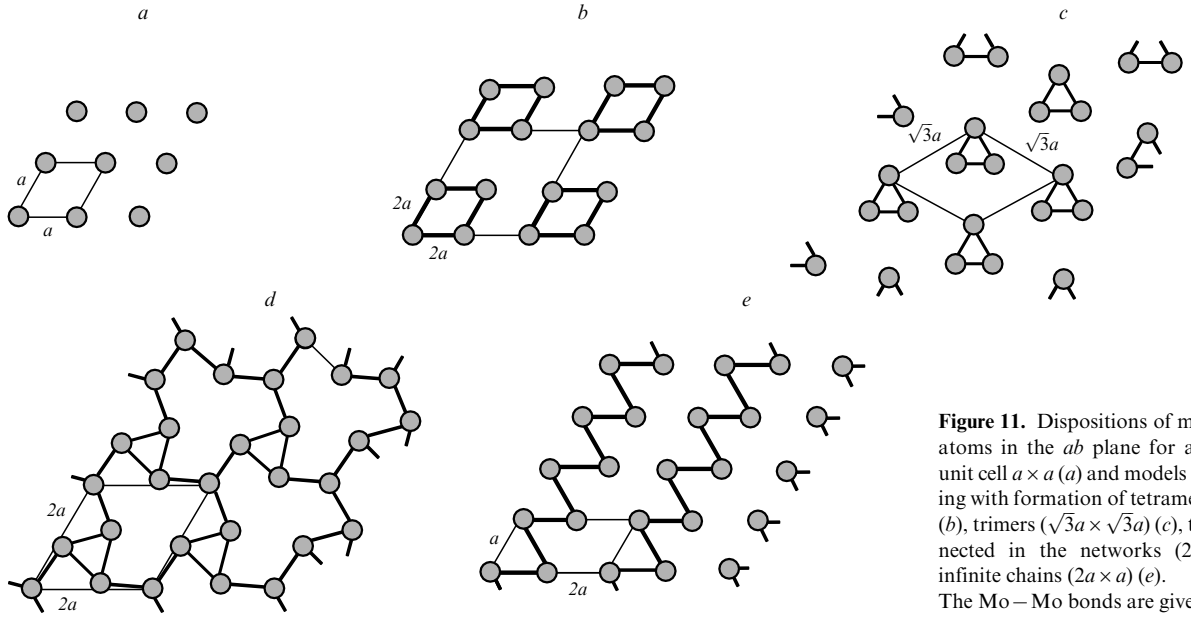


Figure 11. Dispositions of molybdenum atoms in the *ab* plane for a hexagonal unit cell $a \times a$ (*a*) and models of its ordering with formation of tetramers ($2a \times 2a$) (*b*), trimers ($\sqrt{3}a \times \sqrt{3}a$) (*c*), trimers connected in the networks ($2a \times 2a$) (*d*), infinite chains ($2a \times a$) (*e*).
The Mo–Mo bonds are given in bold.

ution of the Mo–Mo distances and the superstructure $2a \times 2a$ were also observed in the MoS_2 layered compounds with intercalated metal hydroxides [157, 158] and metals (Cu, Ag) [165] obtained from dispersions. For the latter compounds, the comparison of X-ray diffraction and electron diffraction data showed that the $2a \times 2a$ superstructure was characteristic of most particles of the sample, however, yet another type of a superstructure, namely, $\sqrt{3}a \times \sqrt{3}a$ was present. The latter type of ordering, also found by scanning tunneling microscopy and electron diffraction in 1T-MoS_2 [the oxidation product of the layered solvates $K_x(H_2O)_yMoS_2$ (see Ref. 32 and 33)], can be described as a result of trimerisation of the molybdenum atoms giving triangular clusters (Fig. 11 *c*).

Based on the data obtained by EXAFS and electron diffraction for the precipitated MoS_2 dispersion, another variant of the cluster-like ordering of molybdenum atoms was proposed (Fig. 11 *d*).[64] This model assumes the displacement of molybdenum atoms in the *ab* plane of the 2H-MoS_2 layer by ~ 0.5 Å to form a trigonal unit cell (space group $P3$, $a = 6.5$ Å) containing 2 and 4 independent molybdenum and sulfur atoms, respectively. Thus, this type of ordering can be considered as being derived from a $2a \times a$ superstructure in the hexagonal cell. It is worth noting that the above-considered models imply an existence of only two M–M distances in the matrix layer, the short and the long (2.8 and 3.8 Å for MoS_2 derivatives), and do not imply the intermediate distance (~ 3.2 Å) which is usually detected by EXAFS in the products precipitated from dispersions. This contradiction can be caused by the inhomogeneity of the nanomaterials in which both distorted and non-distorted fragments of the layers are present [64] or by the inadequacy of the models.

Based on the data from scanning tunnelling microscopy for the MoS_2 films precipitated from the dispersions,[111, 173] a less symmetrical model of the atom ordering which includes the formation of infinite chains (Fig. 11 *e*) was proposed. This type of ordering can be described by using *2a* and *a* as the periods of translation along the *a*- and *b*-axis of the initial hexagonal structure or by taking an orthorhombic unit cell with the parameters $\sqrt{3}a \times a$ in the *ab* plane (where *a* is a parameter of the initial hexagonal cell). It should be mentioned that this type of superstructure was found by scanning tunnelling microscopy and electron microdiffraction also in the layered solvates with potassium $K_x(H_2O)_yMoS_2$ at $0 < x < 0.3$.[32, 33] Based on the analysis of electronograms, a similar type of ordering was proposed for precipitated MoS_2 and WS_2.[169] In this case, the symmetry of the layer was described using a two-dimensional group *pg* and the following parameters for the unit cell (for MoS_2): $a = 5.47$ Å, $b = 3.16$ Å, $\gamma = 90°$ This corresponds to the shortest Mo–Mo distance of 2.92 Å, which is larger by ~ 0.1 Å than the distance inferred from the EXAFS spectra. In the electronograms of the multi-layered particles of the materials studied, the same authors [169] often observed a hexagonal $2a \times 2a$ superstructure which can appear due to stacking of three orthorhombic $\sqrt{3}a \times a$ structures rotated by 120° with respect to each other.

It is of note that only displacements of the molybdenum atoms in the *ab* plane are allowed for in the above-considered models. Meantime, the well established metal dichalcogenide structures are known, where the CDW modulations lead to puckering of the TX_2 layers. An example is given by the rhenium diselenide structure [174] representing a strongly distorted 1T polymorph with puckered layers (space group $P\bar{1}$, $a = 6.72$ Å, $b = 6.60$ Å, $c = 6.73$ Å, $\alpha = 104.9°$, $\beta = 91.8°$, $\gamma = 118.9°$). The mean deviation of the rhenium atoms from the layer plane is ~ 0.1 Å. The rhenium atoms have a strongly distorted octahedral environment consisting of selenium atoms (interatomic Re–Se distances are in the range of 2.35–2.66 Å), and form zigzag chains of irregular Re_4 rhombuses with Re–Re bonds along the *b*-axis. The motif of 'clustering' in $ReSe_2$ is close to that proposed for $LiMoS_2$ based on the calculations and PDF data, though the MoS_2 layer is flat in the latter case.

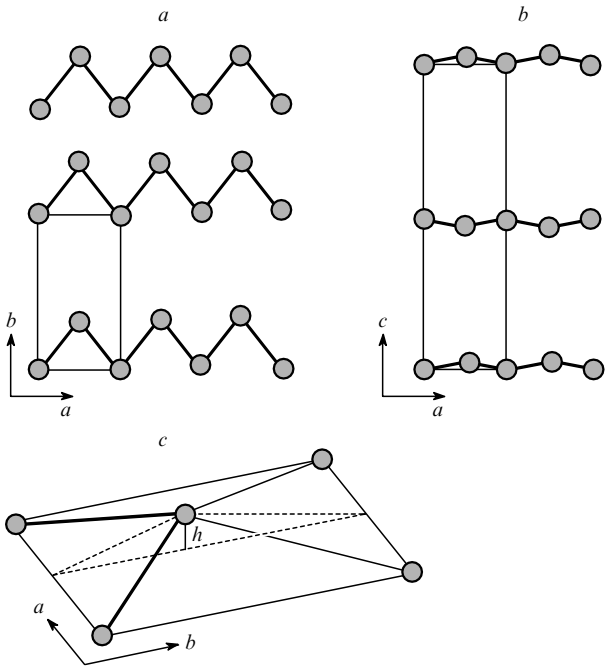


Figure 12. Projections onto the *ab* (*a*) and *ac* (*b*) planes and determination of the parameter of puckering for the T atom layer with puckering of WTe_2 type.

Another type of structure ordering with puckered layers was found for WTe_2 (Ref. 175) in which the tungsten atoms are also in strongly distorted octahedral environment and form infinite chains (Fig. 12 *a*, *b*). Using the model with such puckered layers and considering the diffraction and EXAFS data altogether, the parameters of layer puckering (*h*, in Fig. 12 *c*) were found [106] to be 0.46, 0.45 and 0.09 Å for single-layer dispersions of MoS_2, $MoSe_2$, and WS_2, respectively. It is of note that, upon precipitation of $MoSe_2$ from dispersion, the chains of the atoms are retained in the layer, while the puckering disappears.

In fact, the same type of chain (a structural motif of WTe_2) but a flat variant was earlier used to describe the structure of the precipitated WS_2 on the basis of PDF data analysis.[176] The structure was characterised as monoclinic (space group $P112_1$, $a = 3.27$ Å, $b = 5.71$ Å, $c = 12.31$ Å, $\gamma = 88.48°$). It is important that the existence of all the three metal–metal distances in the distorted layer can be explained employing this model.

Thus, the in-layer structure of the molybdenum- and tungsten-based dichalcogenide matrices dispersed to single layers is modulated by regular distortions with formation of direct metal–metal bonds and these modulations extend for at least tens of Ångstroems. It is noteworthy that the electronic interactions of the initial MoS_2 and $MoSe_2$ matrices with dopant atoms on their surfaces also result in the modulation of their structures, but in this case the modulations are of local character and do not extend for more than one Mo–Mo distance.[177] Note that the variations of superstructure proposed by various researchers may display real dissimilarity in the geometry of the layer in different compounds or even in different particles of the same material. Modification of the layer structure depending on the charge retained on the layer after the formation of the intercalation compound (or, on the time of ageing for precipitation of non-intercalated dichalcogenides TX_2) appears to be quite probable. This follows, for instance, from the difference in the layer geometry between the dispersed and precipitated $MoSe_2$,[106] as well as from the dependence of the relation between three Mo–Mo distances on the guest content, which has been found in the study of a large series of MoS_2 compounds with various guests.[178]

VII. Possible applications of the materials obtained with the use of single-layer dispersions

Layered nanostructured TS_2-based materials prepared through single-layer dispersions have considerable potential in heterogeneous catalysis,[179–185] as lubricants,[186] reagents for the extraction of heavy metals,[164] chemical sensors,[187] novel magnetic materials,[188, 189] and superconductors.[102]

Currently, highly-dispersed molybdenum disulfide doped with 3d-metals (Co, Ni) is the most efficient commercial catalyst for oil hydrorefining. That is why the attempts to use the materials based on the re-precipitated MoS_2 in the hydrodesulfurisation processes appears to be justified.[180, 190] Moreover, these materials were proposed as highly active and selective catalysts for hydrogenation of carbon monoxide to methane [181, 184] and for coal liquefaction.[183] The increase in activity of the Pt/Al_2O_3 supported catalysts of methane oxidation are also achieved with the MoS_2 monolayer deposited onto the Al_2O_3 particles.[185]

In industry, pure molybdenum disulfide has a large-tonnage application as the base for antifriction composites and solid lubricants exploited in wide temperature and pressure ranges as well as in chemically corrosive media and vacuum. Intercalation of MoS_2 with organic compounds, which has become possible with the advent of the single-layer dispersion technique, allows preparation of tribomaterials with enhanced properties as compared with those of materials obtained by mixing the components in the same composition.[186] An approach to produce magnetic lubricants for ferromagnetic surfaces based on the precipitated molybdenum disulfide doped with 3d-metals appears to be of interest.[191]

The single-layer dispersions of MoS_2 are able to bind the heavy-metal cations (first of all, Hg^{2+}) and thus can be considered as potential extractants, for instance, in waste-water purification.[164] In this case, the original MoS_2 and metallic mercury can easily be regenerated on heating the Hg_xMoS_2 formed at relatively low temperature (~ 400 °C) under vacuum, and molybdenum disulfide can be repeatedly used in, at least, 3–5 working cycles with retention of its binding capacity.

It was proposed [187] to use thin partially crystalline, oriented MoS_2 films supported on Al_2O_3 and doped with platinum metals in sensitive and selective detectors of molecular hydrogen. Electroconductivity of such films depends linearly on the concentration of H_2 in the environment. Unlike the traditional sensors based on semiconducting transition-metal oxides, the systems mentioned can operate in the temperature range of 25–150 °C. They are stable in many oxidising and reducing gaseous media.

Upon thermolysis of metal-containing intercalation compounds of metal dichalcogenides, nanosized metal clusters distributed within the layered TX_2 matrix are formed. Such materials may exhibit unique magnetic properties and are thus candidates for various applications in microelectronics.[188, 189] In addition, the oriented films in which the interlayer distance can be widely varied are of potential interest for optics, *e.g.*, for developing novel X-ray mirrors and monochromators.[192]

The currently available heterolayered compounds based on TX_2 and polymers have attracted the attention of many researchers as nanostructured conductors and ionic conductors. It has been mentioned that $NbSe_2$-based nanocomposites can be used for designing plastic superconductors.[102]

VIII. Conclusion

At present, the method for intercalation of metal chalcogenides based on their dispersion to single layers has gained acceptance among the techniques of solid-state chemistry. With this method, it is quite easy to construct layered compounds at room temperature using extended TX_2 structural units and the reagents introduced into solution.

It should be mentioned that the studies performed to date have mainly been focused on the synthetic aspects. Their prospects have been showed and the advantages of a single-layer dispersion technique for the synthesis of novel intercalation compounds have been revealed. As shown above, this method permits one to introduce a rather wide variety of the quests in the materials, *viz.*, cations and neutral molecules of organic substances, polymers, polynuclear organometallic complexes, metal cations and metal hydroxide clusters. The method allowed one to extend essentially the range of TX_2-based layered compounds, first of all, the intercalation compounds of molybdenum and tungsten disulfides as well as nanocomposite materials based on different TX_2 and polymers.

Coincident with manifestation of the advantages, the directions of method perfection have been revealed. It appears that they include, in particular, the use of new non-aqueous solvents providing stability to dispersed systems and possibilities of carrying out further operations for 'assembling' layered compounds. In most studies, aqueous (or aqueous-organic) media were used, which imposes special requirements on the nature of the guest. This problem can partly be overcome by performing the reaction in two-phase systems using aqueous media for dispersion and water-immiscible solvents for dissolving the guest. However, the guests sensitive to hydrolytic decomposition cannot be used even in this combination. Besides, such a procedure, which implies the formation of layered compounds on the interface, makes its isolation difficult and was used until now only for the preparation of materials in the form of films.

Yet another direction of method perfection is the enhancement of structural ordering of the compounds obtained. Usually, this is not high because the 'assembling' of layered compounds proceeds under non-equilibrium conditions. This may have the following consequences:

— non-uniformity in filling of the interlayer spaces by the guest and difficulties in the regulation of the chemical composition, especially with a low guest content (typically, the minimum content is limited by the composition for which the system does not yet contain the macroscopic phase of non-intercalated TX_2 under the given conditions of synthesis; besides, the solvent molecules or alkali metal cations can enter into the interlayer space along with the guest molecules);

— turbostratic stacking of the layers;

— in most cases, the impossibility of raising structural ordering of the materials obtained by annealing, because heating even at moderate temperatures (100–200 °C) often initiates structural transformations and deintercalation processes.

It is obvious that further optimisation of the characteristics of the compounds should be conducted taking into account the specific fields of application (*e.g.*, electronics, catalysis, coating production) of each type of material, since the specialists working in these fields make different demands to the degree of ordering of the nanostructures obtained.

It should be noted that information on the structure of novel intercalation compounds is fragmentary. Often, new compounds are characterised by the only structural parameter, *viz.*, by the interlayer spacing expansion obtained from the XRPD data. More detailed studies of the atomic structures of both the intercalated layer and matrix layers are not numerous yet. The investigations of the material morphology are almost absent. Nevertheless, a comprehensive approach applied in some cases allowed one to establish the chemical nature and local structure of the guest layer, to reveal and to analyse distortions of the host matrix induced by intercalation and to propose the structural models for the studied classes of intercalation compounds not contradicting the body of experimental data.

In our opinion, yet another prospective direction of research exists which has not been sufficiently developed yet. This is the study of the reactivities of two-dimensional structures of TX_2 and the guest in the layered compounds precipitated from dispersions. The ability of such ultra-dispersed systems to undergo chemical transformations may differ essentially from the reactivity of the corresponding components in a bulk sample and this can also be

used for producing novel materials with various practically valuable characteristics.

The research was financially supported by the Russian Foundation for Basic Research (Project No. 00-03-32544) and the Russian Academy of Sciences (in the framework of the programme 'Nanomaterials and supramolecular systems').

References

1. A A Balchi, in *Crystallography and Crystal Chemistry of Materials with Layered Structure* (Ed. F Lévy) (Dordrecht: Reidel, 1976) p. 1
2. A J Jacobson, in *Comprehensive Supramolecular Chemistry* Vol. 7 (Eds G Alberti, T Bein) (New York: Pergamon Press, 1996) p. 315
3. G V Subba Rao, M W Shafer, in *Intercalated Layered Materials* (Ed. F Lévy) (Dordrecht: Reidel, 1979) p. 99
4. R B Somoano, J A Woollam, in *Intercalated Layered Materials* (Ed. F Lévy) (Dordrecht: Reidel, 1979) p. 307
5. R Schöllhorn *Physica B+C* **99** 89 (1980)
6. R Schöllhorn *Inclusion Comp.* **1** 249 (1984)
7. J Rouxel *J. Chim. Phys. Phys.-Chim. Biol.* **83** 841 (1986)
8. R Schöllhorn *Chem. Mater.* **8** 1747 (1996)
9. P Hagenmuller *J. Phys. Chem. Solids* **59** 503 (1998)
10. E Benavente, M A Santa Ana, F Mendizabal, G Gonzalez *Coord. Chem. Rev.* **224** 87 (2002)
11. J A Wilson, A D Yoffe *Adv. Phys.* **18** 193 (1969)
12. L F Mattheiss *Phys. Rev. B* **8** 3719 (1973)
13. M Kertesz, R Hoffmann *J. Am. Chem. Soc.* **106** 3453 (1984)
14. D E Brown, D J Beerntsen *Acta Crystallogr., Sect. B* **18** 31 (1965)
15. A D Yoffe *Solid State Ionics* **39** 1 (1990)
16. G Gruener, A Zettl *Phys. Rep.* **119** 117 (1985)
17. D Gonbeau, K Dartigeas, L Benoist, G Pfister-Guillouzo, G Ouvrard, A Levasseur *J. Electron Spectrosc. Relat. Phenom.* **83** 45 (1997)
18. M J McKelvy, W S Glaunsinger *Mater. Res. Bull.* **21** 835 (1986)
19. A Amara, Y Frongillo, M J Aubin, S Jandl, J M Lopez-Castilio, J P Gerin *Phys. Rev. B* **36** 6415 (1987)
20. H Martinez, C Auriel, G Pfister-Guillouzo, S F Matar *J. Electron Spectrosc. Relat. Phenom.* **87** 19 (1997)
21. Z Y Wu, S Lemaux, P Moreau, P Gressier, F Lemoigno, G Ouvrard *J. Phys. IV, Colloq. C2* **7** 257 (1997)
22. A R Beal, W Y Liang *Philos. Mag.* **27** 1397 (1973)
23. R G Dickinson, L Pauling *J. Am. Chem. Soc.* **45** 1466 (1923)
24. R E Bell, R E Herfert *J. Am. Chem. Soc.* **79** 3351 (1957)
25. R R Chianelli *Int. Rev. Phys. Chem.* **2** 127 (1982)
26. A York *Chem. Ber.* **36** 40 (2000)
27. R Tenne *Mater. Sci. Forum* **232** 275 (1996)
28. M Nath, C N R Rao *Adv. Mater.* **13** 283 (2001)
29. P A Parilla, A C Dillon, K M Jones, G Riker, D I Schulz, D S Ginley, M J Heben *Nature (London)* **397** 114 (1999)
30. V Chikan, D F Kelley *J. Phys. Chem. B* **106** 3794 (2002)
31. F Wypych, R J Schöllhorn *J. Chem. Soc., Chem. Commun.* 1386 (1992)
32. F Wypych, C Solenthaler, R Prins, Th Weber *J. Solid State Chem.* **144** 430 (1999)
33. F Wypych, T Weber, R Prins *Chem. Mater.* **10** 723 (1998)
34. V Alexiev, R Prins, T Weber *Phys. Chem. Chem. Phys.* **2** 1815 (2000)
35. J Heising, M G Kanatzidis *J. Am. Chem. Soc.* **121** 11720 (1999)
36. D W Murphy, G W Hull Jr *J. Chem. Phys.* **62** 173 (1975)
37. C Liu, O Singh, P Joensen, A E Curzon, R F Frindt *Thin Solid Films* **113** 165 (1984)
38. J Rouxel, in *Intercalated Layered Materials* (Ed. F Lévy) (Dordrecht: Reidel, 1979) p. 201
39. S Lemaux, A S Golub, P Gressier, G Ouvrard *J. Solid State Chem.* **147** 336 (1999)
40. F Wypych, M Tsunoda *Quim. Nova* **16** 543 (1993)
41. A R Beal, J V Acrivos *Philos. Mag. B* **37** 409 (1978)
42. D O'Hare, J C O Evans, A Fogg, S O'Brien *Polyhedron* **19** 297 (2000)
43. A S Golub, Yu A Kaftanova, Yu N Novikov, M E Vol'pin *Izv. Akad. Nauk SSSR, Ser. Khim.* 2627 (1987) [a]
44. F R Gamble, J H Osiecki, M Cais, R Pisharody, F J DiSalvo, T H Gebale *Science* **174** 493 (1971)
45. R Schöllhorn, E Sick, A Weiss *Z. Naturforsch. B* **28** 168 (1973)
46. A Zunger, A J Freeman *Phys. Rev. B* **16** 906 (1977)
47. J V Acrivos, J R Salem *Philos. Mag.* **30** 603 (1974)
48. H Ogata, H Fujimori, S Miyajima, K Kobashi, T Chiba, R E Taylor, K Endo *J. Phys. Chem. Solids* **58** 701 (1997)
49. R Schöllhorn, H D Zagefka, T Butz, A Lerf *Mater. Res. Bull.* **14** 369 (1979)
50. M J McKelvy, W S Glaunsinger *J. Solid State Chem.* **67** 142 (1987)
51. M A Le Blanc, M Danot, R Trichet, J Rouxel *Mater. Res. Bull.* **9** 191 (1974)
52. W Rüdorff *Angew. Chem.* **71** 487 (1959)
53. R Schöllhorn, M Kuempers, D Plorin *J. Less-Common Met.* **58** 55 (1978)
54. M G Kanatzidis, T J Marks *Inorg. Chem.* **9** 783 (1987)
55. M B Dines *Mater. Res. Bull.* **10** 287 (1975)
56. M Remskar, A Popovic, H I Starnberg *Surf. Sci.* **430** 199 (1999)
57. M A Py, R R Haering *Can. J. Phys.* **61** 76 (1983)
58. B G Silbernagel, M S Whittingham *J. Chem. Phys.* **64** 3670 (1976)
59. R L Kleinberg *Phys. Chem. Solids* **43** 285 (1982)
60. R L Barinskii, E P Shevchenko, I M Kulikova, A S Golub, Yu N Novikov, M E Vol'pin *Dokl. Akad. Nauk SSSR* **274** 1381 (1984) [b]
61. R H Friend, A D Yoffe *Adv. Phys.* **36** 1 (1987)
62. P Ganal, W Olberding, T Butz, G Ouvrard *Solid State Ionics* **59** 313 (1993)
63. K Chrissafis, M Zamani, K Kambas, J Stoemenos, N A Economu *Mater. Sci. Eng., B* **3** 145 (1989)
64. K E Dungey, M D Curtis, J E Penner-Hahn *Chem. Mater.* **10** 2152 (1998)
65. V Petkov, S J L Billinge, P Larson, S D Mahanti, T Vogt, K K Rangan, M G Kanatzidis *Phys. Rev. B* **65** 92102 (2002)
66. A Lerf, R Schöllhorn *Inorg. Chem.* **16** 2950 (1977)
67. R Schöllhorn, A Weiss *J. Less-Common Met.* **36** 229 (1974)
68. J O Besenhard, H Meyer, R Schöllhorn *Z. Naturforsch. B* **31** 907 (1976)
69. C Lui, O Joensen, A E Curzon, R F Frindt *Thin Solid Films* **113** 165 (1984)
70. F Wypych, M Tsunoda *Quim. Nova* **17** 9 (1994)
71. V Alexiev, H Meyer zu Altenschildesche, R Prins, Th Weber *Chem. Mater.* **11** 1742 (1999)
72. Y Arnaud, M Chevreton, A Ahouandjinou, M Danot, J Rouxel *J. Solid State Chem.* **18** 9 (1976)
73. M Danot, R Brec *Acta Crystallogr., Sect. B* **31** 1674 (1975)
74. J W Lyding, M T Ratajack, C R Kannewurf, W H Goodman, J A Ibers *J. Phys. Chem. Solids* **43** 599 (1982)
75. H J M Bouwmeester *Solid State Ionics* **16** 163 (1985)
76. W Abriel, A Lerf *Mater. Res. Bull.* **23** 673 (1988)
77. H J M Bouwmeester, A van der Lee, S van Smaalen, G A Wiegers *Phys. Rev. B* **43** 9431 (1990)
78. M Danot, J Rouxel *C. R. Seances Acad. Sci., Ser. C* **271** 998 (1970)
79. J Rouxel, A LeBlanc, A Royer *Bull. Soc. Chim. Fr.* 2019 (1971)
80. V S Pervov, V V Volkov, E V Makhonina, A Yu Zavrazhnov, D N Turchen *Neorg. Mater.* **35** 416 (1999) [c]
81. L G Akselrud, J Andre, L M Kulikov, G A Takzei, A A Semenov-Kobzar, L P Romaka *Neorg. Mater.* **34** 489 (1998) [c]
82. Yu L Slovokhotov, Y V Zubavichus, A S Golub, Yu N Novikov, L G Akselrud, L M Kulikov, A A Semenov-Kobzar *Nucl. Instrum. Methods Phys. Res., Sect. A* **470** 295 (2001)
83. R Chevrel, M Sergent, J Prigent *C. R. Seances Acad. Sci., Ser. C* **267** 1135 (1968)
84. J M Van den Berg *Inorg. Chim. Acta* **2** 216 (1968)
85. K Anzenhofer, J J de Boer *Acta Crystallogr., Sect. B* **25** 1419 (1969)
86. J Guillevic, R Chevrel, M Sergent *Bull. Soc. Fr. Mineral Cristallogr.* **93** 495 (1970)
87. J Guillevic, J Y LeMarouille, D Grandjean *Acta Crystallogr., Sect. B* **30** 111 (1974)
88. H Wada, M Onada, H Nozaki, I Kawada *J. Solid State Chem.* **63** 369 (1986)
89. M P Vaqueiro, M L Kosidowski, A V Powell *Chem. Mater.* **14** 1201 (2002)
90. S K S Astava, B Avasthi *Synth. Met.* **11** 193 (1985)

91. N V Elizarova, V S Pervov, A T Fal'kengof, E V Makhonina, B M Zhigarnovskii *Zh. Neorg. Khim.* **39** 1061 (1994) [d]
92. M Danot, J Rouxel, O Gorochov *Mater. Res. Bull.* **9** 1383 (1974)
93. M A Buhanic, P Colombet, M Danot *Solid State Commun.* **59** 77 (1986)
94. Y Kuroiwa, M Nishimura, R Nakajima, H Abe, Y Noda *J. Phys. Soc. Jpn.* **63** 4278 (1994)
95. E W Ong, M J McKelvy, G Ouvrard *Chem. Mater.* **4** 14 (1992)
96. P Moreau, P Canal, G Ouvrard *Mol. Cryst. Liq. Cryst.* **244** 325 (1994)
97. P Moreau, P Canal, A M Marie, G Ouvrard *Inorg. Chem.* **34** 5496 (1995)
98. P Lagrange, M El Marrini, A Herold *Rev. Chim. Mingr.* **20** 229 (1983)
99. N V Pervukhina, S A Magarill, S V Borisov, G V Romanenko, N A Pal'chik *Usp. Khim.* **68** 683 (1999) [*Russ. Chem. Rev.* **68** 615 (1999)]
100. P Joensen, R F Frindt, S R Morrison *Mater. Res. Bull.* **21** 457 (1986)
101. J P Lemmon, J Wu, C Oriakhi, M M Lerner *Electrochim. Acta* **40** 2245 (1995)
102. H L Tsai, J L Schindler, C R Kannewurf, M G Kanatzidis *Chem. Mater.* **9** 875 (1997)
103. L Wang, M G Kanatzidis *Chem. Mater.* **13** 3717 (2001)
104. B K Miremadi, S R Morrison *J. Appl. Phys.* **63** 4970 (1988)
105. D Yang, R F Frindt *J. Phys. Chem. Solids* **57** 1113 (1996)
106. R A Gordon, D Yang, E D Crozier, D T Jiang, R F Frindt *Phys. Rev. B* **65** 125407 (2002)
107. D Yang, S Jiménez-Sandoval, W M R Divigalpitiya, J C Irwin, R F Frindt *Phys. Rev. B* **43** 12053 (1991)
108. D Yang, R F Frindt *Mol. Cryst. Liq. Cryst. Sci. Technol., Sect. A* **244** 355 (1994)
109. P Joensen, E D Crozier, N Alberding, R F Frindt *J. Phys. C* **20** 4043 (1987)
110. S Jiménez-Sandoval, D Yang, R F Frindt, J C Irwin *Phys. Rev. B* **44** 3955 (1991)
111. X R Qin, D Yang, R F Frindt, J C Irwin *Ultramicroscopy* **42–44** 630 (1992)
112. D Yang, R F Frindt *J. Appl. Phys.* **79** 2376 (1996)
113. A V Powell, L Kosidowski, A McDowall *J. Mater. Chem.* **11** 1086 (2001)
114. R Bissessur, J Heising, W Hirpo, M Kanatzidis *Chem. Mater.* **8** 318 (1996)
115. A S Golub, G A Protsenko, L V Gumileva, A G Buyanovskaya, Yu N Novikov *Izv. Akad. Nauk, Ser. Khim.* **4** 672 (1993) [a]
116. M Danot, J L Mansot, A S Golub, G A Protzenko, P B Fabritchnyi, Yu N Novikov, J Rouxel *Mater. Res. Bull.* **29** 833 (1994)
117. B K Miremadi, T Cowan, S R Morison *J. Appl. Phys.* **69** 6373 (1991)
118. W M R Divigalpitiya, R F Frindt, S R Morrison *Science* **246** 369 (1989)
119. D Guay, W M R Divigalpitiya, D Belanger, X H Feng *Chem. Mater.* **6** 614 (1994)
120. X Zhou, D Yang, R F Frindt *J. Phys. Chem. Solids* **57** 1137 (1996)
121. H Tagaya, T Hashimoto, M Karasu, T Izumi, K Chiba *Chem. Lett.* **12** 2113 (1991)
122. V Sanchez, E Benavente, M A Santa Ana, G Gonzalez *Chem. Mater.* **11** 2296 (1999)
123. L Kosidowski, A V Powell *Chem. Commun.* 2201 (1998)
124. J Heising, F Bonhomme, M G Kanatzidis *J. Solid State Chem.* **139** 22 (1998)
125. L F Nazar, A J Jacobson *J. Chem. Soc., Chem. Commun.* 570 (1986)
126. L F Nazar, A J Jacobson *J. Mater. Chem.* **4** 1419 (1994)
127. A S Golub, Ya V Zubavichus, Yu L Slovokhotov, Yu N Novikov, M Danot *Solid State Ionics* **128** 151 (2000)
128. A S Golub, I B Shumilova, Yu N Novikov, J L Mansot, M Danot *Solid State Ionics* **91** 307 (1996)
129. R Bissessur, R I Haines, D R Hutchings, R Bruning *Chem. Commun.* 1598 (2001)
130. A Golub, G Protzenko, I Shumilova, Y Zubavichus, C Payen, Yu Novikov, M Danot *Mol. Cryst. Liq. Cryst.* **311** 377 (1998)
131. S Nakagaki, A S Mangrich, F Wypych *Inorg. Chim. Acta* **254** 213 (1997)
132. A S Golub, I B Shumilova, Y V Zubavichus, M Jahncke, G Smss-Fink, M Danot, Yu N Novikov *J. Mater. Chem.* **7** 163 (1997)
133. J Brenner, C L Marshall, L Ellis, N Tomczyk, J Heising, M Kanatzidis *Chem. Mater.* **10** 1244 (1998)
134. N Lara, E Ruiz-Hitzky *J. Braz. Chem. Soc.* **7** 193 (1996)
135. M G Kanatzidis, R Bissessur, D C DeGroot, J L Schindler, C R Kannewurf *Chem. Mater.* **5** 595 (1993)
136. R Bissessur, M G Kanatzidis, J L Schindler, C R Kannewurf *J. Chem. Soc., Chem. Commun.* 1582 (1993)
137. E Ruiz-Hitzky, R Jimenez, B Casal, V Manriquez, A Santa Ana, G Gonzalez *Adv. Mater.* **5** 738 (1993)
138. R Bissessur, J L Schindler, C R Kannewurf, M Kanatzidis *Mol. Cryst. Liq. Cryst.* **245** 249 (1994)
139. J P Lemmon, M M Lerner *Chem. Mater.* **6** 207 (1994)
140. F Wypych, L B Adad, M C Grothe *Quim. Nova* **21** 687 (1998)
141. F Wypych, N Seefeld, I Denicolo *Quim. Nova* **20** 356 (1997)
142. D Yang, P Westreich, R F Frindt *Nanostruct. Mater.* **12** 467 (1999)
143. P J Ollivier, N I Kovtyukhova, S W Keller, T E Mallout *Chem. Commun.* 1563 (1998)
144. D J Harris, T J Bonagamba, K Schmidt-Rohr *Macromolecules* **32** 6718 (1999)
145. G Gonzales, M A Santa Ana, E Benavente *Electrochim. Acta* **43** 1327 (1998)
146. L Hernan, J Morales, J Santos *J. Solid State Chem.* **141** 323 (1998)
147. L Wang, J Schindler, J A Thomas, C R Kannewurf, M G Kanatzidis *Chem. Mater.* **7** 1753 (1995)
148. W M R Divigalpitiya, R F Frindt, S R Morrison *J. Mater. Res.* **6** 1103 (1991)
149. A D Pomogailo *Usp. Khim.* **69** 60 (2000) [*Russ. Chem. Rev.* **69** 53 (2000)]
150. V S Pervov, E V Makhonina *Usp. Khim.* **69** 528 (2000) [*Russ. Chem. Rev.* **69** 481 (2000)]
151. P Aranda, E Ruiz-Hitzky *Chem. Mater.* **4** 1395 (1992)
152. M B Armand *Adv. Mater.* **2** 278 (1990)
153. M A Gee, R F Frindt, P Joensen, S R Morrison *Mater. Res. Bull.* **21** 543 (1986)
154. A S Golub, Ya V Zubavichus, N D Lenenko, Yu L Slovokhotov, M Dano, Yu N Novikov *Izv. Akad. Nauk, Ser. Khim.* 2191 (2001) [a]
155. A S Golub, G A Protzenko, I M Yanovskaya, O L Lependina, Yu N Novikov *Mendeleev Commun.* 199 (1993)
156. E F Valeev, Ya V Zubavichus, Yu L Slovokhotov, A S Golub, G A Protzenko, Yu N Novikov *Physica B* **208–209** 569 (1995)
157. Y V Zubavichus, A S Golub, Y N Novikov, Y L Slovokhotov, P J Schilling, R C Tittsworth *J. Phys. IV, Colloq. C2* **7** 1057 (1997)
158. Y V Zubavichus, Yu L Slovokhotov, P J Schilling, R C Tittsworth, A S Golub, G A Protzenko, Yu N Novikov *Inorg. Chim. Acta* **280** 211 (1998)
159. A F Wells *Structural Inorganic Chemistry* (Oxford: Oxford University Press, 1986)
160. M Danot, M I Afanasov, P B Fabritchnyi, A S Golub, N D Lenenko, Y N Novikov, K V Pokholov, I A Presniakov *Solid State Ionics* **128** 211 (2000)
161. M I Afanasov, M Dano, P B Fabrichnyi, A S Golub, N D Lenenko, Yu N Novikov, K V Pokholok, I A Presnyakov *Zh. Neorg. Khim.* **45** 857 (2000) [d]
162. A S Golub, C Payen, G A Protzenko, Yu N Novikov, M Danot *Solid State Commun.* **102** 419 (1997)
163. Y V Zubavichus, A S Golub, N D Lenenko, Yu L Slovokhotov, Yu N Novikov, M Danot *Mater. Res. Bull.* **34** 1601 (1999)
164. A E Gash, A L Spain, L M Dysleski, C J Flashenreim, A Kalaveshi, P K Dorhout, S H Strauss *Environ. Sci. Technol.* **32** 1007 (1998)
165. A S Golub, I B Shumilova, Y V Zubavichus, Yu L Slovokhotov, Yu N Novikov, A M Marie, M Danot *Solid State Ionics* **122** 137 (1999)

166. P G Allen, A E Gach, P K Dorhout, S H Strauss *Chem. Mater.* **13** 2257 (2001)
167. M Francois, W Lengauer, K Yvon, H B Yaich-Aerrache, P Gougeon, M Potel, M M Sergent *Z. Kristallogr.* **196** 111 (1991)
168. Ya V Zubavichus, Candidate Thesis in Chemical Sciences, Institute of Organoelement Compounds, Russian Academy of Sciences, Moscow, 2001
169. J Heising, M G Kanatzidis *J. Am. Chem. Soc.* **121** 638 (1999)
170. C Rovira, M-H Whangbo *Inorg. Chem.* **32** 4094 (1993)
171. M H Whangbo, E Canadell *J. Am. Chem. Soc.* **114** 9587 (1992)
172. X Rocquefelte, F Boucher, P Gressier, G Ouvrard *Phys. Rev. B* **62** 2397 (2000)
173. X R Qin, D Yang, R F Frindt, J C Irwin *Phys. Rev. B* **44** 3490 (1991)
174. J C Wildervanck, F Jellinek *J. Less-Common Met.* **24** 73 (1971)
175. A Mar, S Jobic, J A Ibers *J. Am. Chem. Soc.* **114** 8963 (1992)
176. V Petkov, S J L Billinge, J Heising, M G Kanatzidis *J. Am. Chem. Soc.* **122** 11 571 (2000)
177. K Kataoka, H Murata, A Koma *Surf. Sci.* **478** 131 (2001)
178. Ya V Zubavichus, A S Golub, N D Lenenko, Yu N Novikov, Yu L Slovokhotov, M Danot *J. Mol. Catal. A: Chem.* **158** 231 (2000)
179. M D Curtis, M David, H Willard *ACS Symp. Ser.* **653** 154 (1996)
180. K E Dungey, M D Curtis, J E Penner-Hahn *J. Catal.* **175** 129 (1998)
181. B K Miremadi, S R Morrison *J. Catal.* **103** 334 (1987)
182. M D Valle, M Avalos-Borja, J Cruz, S Fuentes *Mater. Res. Soc. Symp. Proc.* **351** 287 (1994)
183. B C Bockrath, D S Parfitt *Catal. Lett.* **33** 201 (1995)
184. G A Scholz, S R Morrison *Can. J. Chem.* **67** 862 (1989)
185. B K Miremadi, S R Morrison *J. Catal.* **131** 127 (1991)
186. A P Krasnov, O V Afonicheva, V A Mit', A S Golub, I B Shumilova, Yu N Novikov *Trenie Iznos* **17** 799 (1996)
187. B K Miremadi, R C Singh, S R Morrison, K Colbow *Appl. Phys. A* **63** 271 (1996)
188. R F Frindt, A S Arrott, A E Curzon, B Heinrich, S R Morrison, T L Templeton, R Divigalpitiya, M A Gee, P Joensen *J. Appl. Phys.* **70** 6224 (1991)
189. T L Templeton, A S Arrott, A E Curzon, M A Gee, X Z Li, Y Yoshida, P J Schurer, J L LaCombe *J. Appl. Phys.* **73** 6668 (1993)
190. W P Boone, J G Ekerdt *J. Catal.* **193** 96 (2000)
191. B K Miremadi, K Colbow, S R Morrison *J. Appl. Phys.* **82** 2636 (1997)
192. W M R Divigalpitiya, R F Frindt, S R Morrison *Appl. Surf. Sci.* **48–49** 572 (1991)

[a] — *Russ. Chem. Bull., Int. Ed. (Engl. Transl.)*
[b] — *Dokl. Chem. (Engl. Transl.)*
[c] — *Inorg. Mater. (Engl. Transl.)*
[d] — *Russ. J. Inorg. Chem. (Engl. Transl.)*